DEVELOPMENT OF CHONDROITIN SULPHATE-BASED SCAFFOLDS TARGETING BONE REGENERATION APPLICATIONS

JÚLIA PISSAIA MATTÉ

Thesis submitted to

Escola de Tecnologia e Gestão – Instituto Politécnico de Bragança

to obtain a master's degree in

Chemical Engineering

Within the context of the double diploma with

Universidade Tecnológica Federal do Paraná

Supervisors

Profª Dra. Filomena Barreiro

Dra. Arantzazu Santamaria Echart

Dra. Yaidelin Manrique

Profª. Dra. Elisângela Düsman

Bragança, Portugal

2024

This work was partially supported by national funds through FCT/MCTES (PIDDAC): CIMO, UIDB/00690/2020 (DOI: 10.54499/UIDB/00690/2020) and UIDP/00690/2020 (DOI: 10.54499/UIDP/00690/2020); SusTEC, LA/P/0007/2020 (DOI: 10.54499/LA/P/0007/2020);); Fundação Araucária and Universidade Tecnológica Federal do Paraná within the context of the project PD&I Nº 429/2022, and Conselho Nacional de Desenvolvimento Científico e Tecnológico (CNPq#305029/2022-3).

ACKNOWLEDGMENTS

The conclusion of this work was possible because I had the support and help of many people throughout this stage. I would like to thank all of you:

To my supervisors, Professor Dr Filomena Barreiro, Dr Arantzazu Santamaria-Echart, Dr Yaidelin Manrique and Professor Dr Elisângela Dusman, I thank you for the opportunity, for the knowledge shared, for your patience and your support during the completion of this work. I would also like to thank Dr Tatiana La Banca Schreiner, who was always there for me and helped me at all times during this research.

I would like to thank the Federal Technological University of Paraná, the professors at the Campus Francisco Beltrão, the Polytechnic Institute of Bragança and its lecturers for the support and opportunities they have given me, making it possible for me to gain a master's degree in Chemical Engineering. I would like to thank the Faculty of Engineering at the University of Porto and the team at the Chemical Engineering laboratories for making it possible to carry out this work. I would also like to thank Evellin and Anna for carrying out the biological analyses.

To my parents, Claudia and Mauro Matté, my eternal gratitude for supporting and encouraging me at every stage of my life. You are my greatest inspiration. To my aunt and uncle, Cristiane and Paulo Pissaia, for always cheering me on. To my grandmothers, Aurora and Dianete, for all their love and care. To my cousins, Guilherme, Isabella, Pietro, Alice and Camila, for being the siblings I never had and for always being by my side. Thanks to all my family for their constant support and affection.

To Andre, for his company, affection, love, and kindness, for making everything easier, and for always being by my side. To my friends, Fernanda, Maria Eduarda, Thais, Mariana, Maria Jhulia, Luan, Denis, and João Vitor, for their friendship and for being there for me even at a distance. To my colleagues in the lab, especially Carlos, Giovana, Maria Clara and Sofia, for making my working days more fun, and for always helping me. To the friends I made in Portugal, especially my friends from Loreto, for their warm welcome and for becoming family in such a short time.

Finally, my sincere thanks to everyone who contributed in some way to the realisation of this work.

ABSTRACT

Bone tissue is a complex biomaterial composed of proteins and minerals essential for the skeleton's structure and function. However, factors such as ageing, trauma, inflammation, and genetic disorders can compromise bone integrity. While bones possess a natural ability to heal, treating defects remains challenging. Innovative approaches are focusing on substances like chondroitin sulphate (CS), chitosan (CH), and hydroxyapatite (HAp) for their beneficial properties. In this study, HAp/CH scaffolds with different CS concentrations were developed, focusing on bone regeneration. The composition of the scaffolds followed the typical proportion of bone, with 70% HAp as the inorganic component and 30% CH as the organic component. This combination mimics the natural bone matrix and is gradually resorbed by the body, facilitating regeneration. Due to the addition of acetic acid for CH dissolution, a purification step was carried out using supercritical CO_2 ($scCO_2$) to remove it from the final material. Thermogravimetric (TG) analyses showed that $scCO_2$ was effective in removing the acid, with extraction yields ranging from 55% to 100%, depending on the sample, confirming the scaffolds' biological viability. Density and swelling analyses were carried out to characterise the samples. The values obtained showed a density of approximately 0.05 g/cm³ and swelling capacities ranging from 2.79 to 3.24 g/g, both in line with the data available in the literature. In addition, Fourier transform infrared spectroscopy (FTIR) analysis was used to identify the functional groups and chemical bonds present in the material, providing a clear view of the molecular composition. Cytotoxicity tests showed that the samples were not toxic within 48 hours. Thus, the results indicated that the scaffolds incorporated with CS showed good structural stability and biological behaviour, making them suitable materials for bone regeneration. In addition, the process of obtaining CS is being studied in the project “Obtaining, characterising and evaluating the bioactive potential of chondroitin sulphate from tilapia scales”, to which this thesis contributes.

Keywords: Scaffolds; Bone regeneration; Chondroitin sulphate; Chitosan; Hydroxyapatite.

RESUMO

O tecido ósseo é um biomaterial complexo, composto de proteínas e minerais essenciais para a estrutura e a função do esqueleto. No entanto, fatores como envelhecimento, trauma, inflamação e distúrbios genéticos podem comprometer a integridade óssea. Embora os ossos tenham uma capacidade natural de se regenerar, o tratamento de defeitos continua a ser um desafio. As abordagens inovadoras estão se concentrando na utilização de substâncias como o sulfato de condroitina (CS), quitosano (CH) e hidroxiapatite (HAp) dado as suas propriedades benéficas. Neste estudo, foram desenvolvidos *scaffolds* de HAp/CH com diferentes concentrações de CS visando aplicações na área da regeneração óssea. A composição dos *scaffolds* baseou-se na proporção típica do osso que inclui 70% de HAp (componente inorgânico) e 30% de CH (componente orgânico). Esta combinação imita a matriz óssea natural e é gradualmente reabsorvida pelo corpo, facilitando a regeneração. Dada a utilização de ácido acético para solubilizar o CH, a purificação dos materiais foi realizado usando CO_2 supercrítico ($scCO_2$). As análises termogravimétricas (TG) mostraram que o $scCO_2$ foi eficaz na remoção do ácido, com rendimentos de extração variando de 55% a 100%, dependendo da amostra, o que aponta para a viabilidade biológica dos *scaffolds*. Para caracterizar as amostras, foram realizadas análises de densidade e inchamento. Os valores obtidos indicaram uma densidade de aproximadamente 0,05 g/cm³ e capacidade de inchamento que variou de 2,79 a 3,24 g/g, ambos os parâmetros de acordo com os dados disponíveis na literatura. Adicionalmente, a análise de espectroscopia de infravermelho por transformada de Fourier (FTIR) foi usada para identificar os grupos funcionais e as ligações químicas presentes no material, fornecendo uma visão clara da composição molecular. Os testes de citotoxicidade mostraram que as amostras não foram tóxicas para um período de 48 horas. Assim, os resultados indicaram que os *scaffolds* incorporados com CS apresentaram boa estabilidade estrutural e comportamento biológico, tornando-os materiais adequados para uso na regeneração óssea. Adicionalmente, o processo de obtenção de CS está sendo alvo de estudos no projeto "Obtenção, caracterização e avaliação do potencial bioativo do sulfato de condroitina de escamas de tilápia", para o qual esta tese contribui.

Palavras-chave: *Scaffolds*; Regeneração óssea; Sulfato de condroitina; Quitosano; Hidroxiapatite.

INDEX

INDEX OF FIGURES

INDEX OF TABLES

LIST OF SYMBOLS AND NOMENCLATURE

ATR	attenuated total reflectance
CH	chitosan
CS	chondroitin sulphate
CV	cell viability
C_w	swelling capacity
DMEM	Dulbecco's modified eagle medium
DMSO	dimethyl sulphoxide
FTIR	Fourier-transform infrared spectroscopy
GAGs	glycosaminoglycans
HAp	hydroxyapatite
MTT	methylthiazolydiphenyl-tetrazolium bromide
nHAp	nano-hydroxyapatite
PBS	phosphate-buffered saline
pH	potential hydrogen
$scCO_2$	supercritical CO_2 treatment
SEM	scanning electron microscopy
TG	thermal degradation
UTFPR	Federal Technological University of Paraná

1 INTRODUCTION

1.1 Motivation

Bone tissue is a complex organ comprising substantial amounts of proteins and minerals. The osteoblast is the cellular source of bone formation and plays a vital role during the evolution of the skeleton. Ageing, trauma, inflammation, or genetic disorders are pathologies that compromise the structure and function of bones (Amiryaghoubi *et al.*, 2022).

Bones generally have a high healing capacity, and defects are naturally limited to dimensions that can regenerate spontaneously under biological stimuli and a favourable microenvironment. However, even with this intrinsic ability, treating bone defects is challenging (Amiryaghoubi *et al.*, 2022; Wang *et al.*, 2022). Because of this, the search for innovative and effective approaches to regenerate and maintain the integrity of bone tissue has gained prominence.

Substances such as chondroitin sulphate (CS), chitosan (CH), and hydroxyapatite (HAp) have excelled in research and studies for bone treatments due to their beneficial properties for bone health. CS can improve bone regeneration by enhancing the effectiveness of the distribution of growth factors crucial to the bone regenerative process (Zhou *et al.*, 2021). CH is a functional biopolymer that can be processed into porous structures for cell transplantation and tissue regeneration (Laranjeira & Fávere, 2009). HAp, a bioceramic material, stands out for having a chemical composition similar to the inorganic portion of bone (Venkatesan *et al.*, 2012). In particular, the use of substances such as CS shows beneficial effects on joint cells and positive clinical results, including a significant reduction in joint space in osteoarthritis, since it has a chondroprotective action, with anti-inflammatory, anti-catabolic and anabolic properties, especially in cartilage cells, the chondrocytes (Ferrari, 2016; Moniz, 2015).

In this context, advances in tissue engineering led to the development of three-dimensional structures called scaffolds, which play a crucial role in bone regeneration. Scaffolds are a temporary matrix for bone growth and provide a specific environment and structure for the tissue, allowing free cell growth on their walls (Wang *et al.*, 2022; Guo *et al.*, 2023).

This context highlights the interconnection between insights into bone diseases, research on substances like CS, CH, and HAp, and progress in tissue engineering technologies, particularly in scaffold development. Exploring these approaches opens up

a promising horizon for therapeutic innovation to improve patient's quality of life affected by debilitating bone conditions.

1.2 Objectives

The main objective of this work is to develop chondroitin sulphate-based scaffolds targeting bone regeneration applications. Different strategies for incorporating chondroitin sulphate can be applied, like the production of micro/nanoparticles or the combination with other materials like CH or HAp, which are widely used for tissue engineering scaffolds. This work is part of the project "Obtainment, characterisation and evaluation of the bioactive potential of chondroitin sulphate from tilapia scales", mainly concentrated on developing the materials and obtaining their physicochemical and morphological properties. The biological characterisations were carried out in cooperation with the Federal Technological University of Paraná (UTFPR).

The specific objectives are:

- Development of base scaffolds produced from nHAp and CH mimicking the bone composition (70% inorganic and 30% organic), which can be used as a benchmark;
- Development of strategies to incorporate the CS into the scaffolds, mainly including the production of hybrid materials;
- Evaluate the physicochemical and morphological properties of the produced scaffolds;
- Proceed with the preliminary biological evaluation of the scaffolds.

This document is organised into five chapters. The first chapter presents the context and objectives of the study. The second chapter covers a scientific literature review on bone defects, the definition and applications of scaffolds, as well as an analysis of the polymers used in this work. The third chapter details the methodologies used to prepare the dispersion, manufacture, purify and characterise the scaffolds developed. The fourth chapter presents the results and discussion related to the experimental work carried out in the thesis. Finally, the fifth chapter summarises the main results achieved and makes suggestions for future studies.

2 BIBLIOGRAPHIC REVIEW

2.1 Bone structure

Bones are complex structures, as shown in Figure 1, composed of hydroxyapatite (60-70%), the inorganic part, and collagen, the organic part (Backes, 2020; Ruphuy *et al.*, 2016; Beu *et al.*, 2017). Apart from supporting the body, bones are the storehouse of minerals essential for other body systems' functioning. Healthy bones are, therefore, critical to a good quality of life.

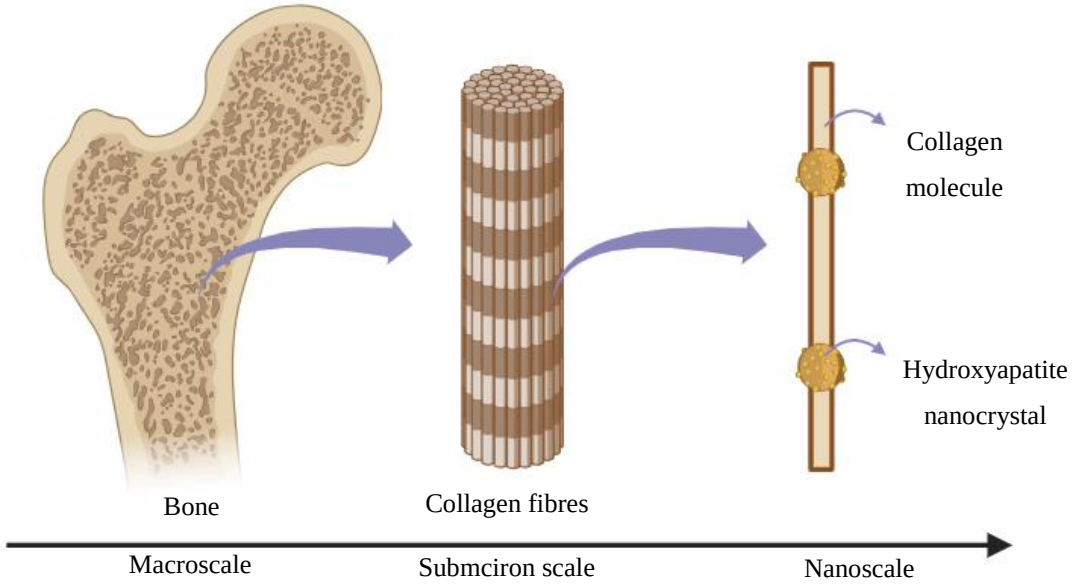

Figure 1 – Schematic diagram of the structure of bone tissue.

Adapted from Ruphuy *et al.*, 2019.

Over time, humans naturally lose part of their bone mass (UNIRIO, 2020). However, from age 50, osteoarticular diseases affect more than 15% of the world's population, and there is no cure (Cruz, 2021). Osteoarticular diseases refer to various conditions affecting the joints, bones, muscles, tendons and ligaments. These conditions can result from several factors, including ageing, natural wear and tear on the joints, injuries, inflammation and genetic predisposition, such as osteoarthritis, a chronic disease that causes articular cartilage degeneration (Rezende *et al.*, 2013).

Bone grafts have been implanted for many years, and despite being a widely used technique, the number of donor sites is low, and there may be scars that require a longer recovery time, increasing the risk of possible infections (Ruphuy *et al.*, 2018). As a result, structures are being developed to mimic the organic and inorganic composition of bones, with characteristics similar to these materials, i.e., able to withstand tension and have adequate porosity to transport nutrients (Backes, 2020; Ruphuy *et al.*, 2016).

2.2 Scaffolds

Bones have a high capacity for regeneration. However, depending on the extent of the damage, this capacity is limited (Miri *et al.*, 2024). Given this, scaffolds are being used for bone regeneration. These structures provide mechanical support and act as cell growth regulators, allowing nutrients and metabolites to pass through. To produce materials as similar as possible to the structure of the natural extracellular matrix of tissues, enabling the attachment, proliferation and differentiation of cells, different methods are being studied to produce scaffolds important for promoting cell growth and the development of tissues similar to that produced naturally by the body (Backes, 2020; Flores *et al.*, 2023).

Among the studied methods, electrospinning and 3D bioprinting can be highlighted. The latter ensures the obtainment of scaffolds with more rigid structures and better mechanical properties (Flores *et al.*, 2023). In addition, different materials can be used to produce them, such as metals, ceramics, and polymers (Backes, 2020).

There is also the production of scaffolds using the freeze-drying technique, making it possible to prepare three-dimensional porous structures with a porosity of over 90% and a pore diameter range of 20-400 μm (Fereshteh, 2018). This approach creates bioactive scaffolds to generate scaffolds in flat, three-dimensional geometries (Brougham *et al.*, 2017).

To be used as a structure for bone regeneration, scaffolds must be versatile, and customisable but also biocompatible and biodegradable, presenting bioactivity, high porosity, good mechanical properties and structural stability (Miri *et al.*, 2024).

When produced with CS and other compounds, such as CH or HAp, scaffolds have the potential to accelerate the bone repair process and have positive effects on inhibiting inflammation, as well as increasing bone hardness (Guo *et al.*, 2023; Xu *et al.*, 2021).

2.3 Hydroxyapatite

HAp, with the chemical formula $Ca_{10}(PO_4)_6(OH)_2$, is a calcium phosphate biomaterial, as shown in Figure 2 (Valentim *et al.*, 2018). It can be chemically synthesised or extracted from natural sources such as cattle, fish, eggs, and pig bones (Wang *et al.*, 2024; Rstakyan *et al.*, 2024).

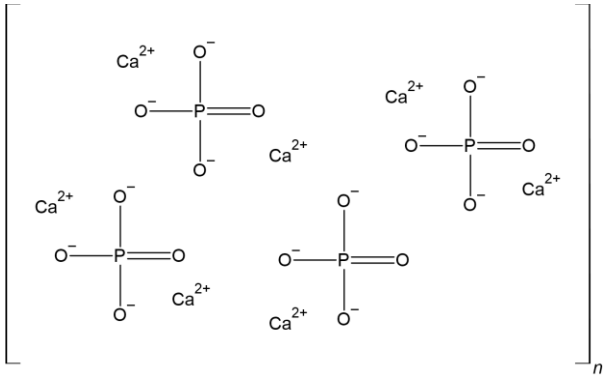

Figure 2 – Chemical structure of HAp.

Synthetic HAp comprises calcium and phosphorus, with a Ca/P ratio of 1.67. Compared to synthetic HAp, natural HAp does not follow a strict stoichiometry, as it includes trace elements such as Mg^{2+}, Zn^{2+}, Cu^{2+}, F, Se^{2+}, Si^{2+}, B^{3+}, giving it a closer resemblance to the chemical composition of human bone (Rstakyan *et al.*, 2024).

Due to this compatibility with human bone, its main constituent, its bioactivity and mechanical strength, HAp has been widely studied in various areas of biomedical applications (Janek *et al.*, 2024; Hu *et al.*, 2017). This content will be explained in the next section.

2.3.1 Applications of nHAp

Nano-hydroxyapatite (nHAp) is more beneficial than conventional HAp in terms of stimulating osteoblast adhesion, differentiation and proliferation, as well as for promoting osseointegration and the deposition of calcium-containing minerals on its surface (Ruphuy *et al.*, 2016). For this reason, nHAp scaffolds combined with other materials, such as polylactic acid, CH, CS, and others, have been reported to have the ability to provide an environment conducive to cell adhesion and development, favouring the reconstruction of orthopaedic defects (Hu *et al.*, 2017). Table 1 shows the main forms and applications of nHAp and HAp.

Table 1 – Main forms and applications of nHAp and HAp.

Compounds	Application	Reference
Nano-hydroxyapatite + Chitosan	Inorganic-organic hybrid materials for biomedical applications	Ruphuy *et al.*, 2016
Hydroxyapatite + Chitosan + Amylopectin + Chondroitin Sulphate	Scaffolds for bone tissue engineering	Venkatesan *et al.*, 2012
Nano-hydroxyapatite + Chitosan + Chondroitin Sulphate + Hyaluronic acid	Biomimetic mineralized hybrid scaffolds for bone tissue engineering	Hu *et al.*, 2017
Nano-hydroxyapatite + Polylactic acid + Magnesium nano-oxide	3D-printed scaffolds for bone defect repair	Xu *et al.*, 2022
Nano-hydroxyapatite + Gelatine + Chitosan + Polyvinyl alcohol	Biomimetic scaffolds for bone tissue engineering	Ma *et al.*, 2021

The studies by Ma *et al.* (2021) and Venkatesan *et al.* (2012) were highlighted because they presented the best results. For example, in the work carried out by Ma *et al.* (2021), promising biomimetic scaffolds for tissue engineering were developed. The nHAp, in addition to improving the mechanical properties of the scaffolds, also promoted cell adhesion on hydrophilic surfaces. Venkatesan *et al.* (2012) demonstrated the preparation of promising biomaterials-based scaffolds in tissue engineering, as they presented excellent interconnected porosity, controlled biodegradation and enhanced cell proliferation.

2.4 Chitosan

CH is the only alkaline polysaccharide among natural polysaccharides and is produced by the de-N-acetylation of chitin (Wang *et al.*, 2024). It is a biomaterial with a chemical structure (Figure 3) that resembles glycosaminoglycans (GAGs) and has advantageous properties such as biodegradability, biocompatibility and hydrophilicity (Wang *et al.*, 2024; Xu *et al.*, 2020).

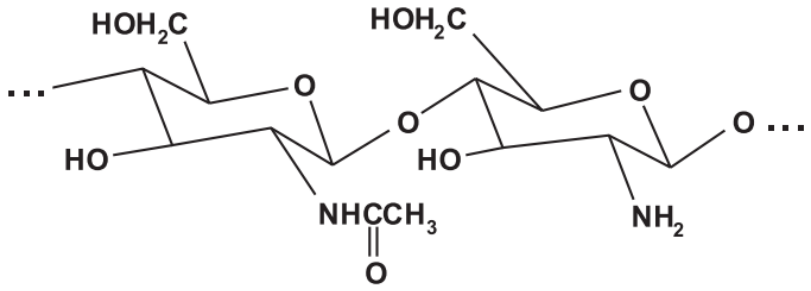

Figure 3 – Chemical structure of CH.

Adapted from Laranjeira & Fávere, 2009.

Due to its biomimetic properties and remarkable degradability, CH has emerged as a versatile choice for developing scaffolds, dressings and controlled drug release systems. In addition, it can stimulate tissue regeneration and repair through various mechanisms, including the increase of cell adhesion and promoting angiogenesis, resulting in a significant acceleration of the skin regeneration process (Wang *et al.*, 2024).

In solution, CH acquires a cationic charge, which enables the formation of polyelectrolyte complexes (PECs) with anionic polymers through electrostatic interactions (Xu *et al.*, 2020). CH contains amino and hydroxyl groups, which are active functional groups susceptible to chemical reactions, making them readily modifiable (Wang *et al.*, 2024).

2.4.1 Applications of CH

As it is a non-toxic, bioactive, biocompatible polymer with adsorption capacity and chelating ability, CH can be used in different areas of application, such as agriculture, tissue engineering, pharmaceuticals, the food industry and effluent treatment (Felipe *et al.*, 2017). Table 2 shows the main forms and applications of materials containing CH.

Table 2 – Main forms and applications of CH-containing materials.

Compounds	Application	Reference
Chitosan + Chondroitin Sulphate	Encapsulation of proanthocyanidin for food preservation	Yu *et al.*, 2022
Chitosan + Chondroitin Sulphate	Microcapsules for the controlled release of 5-fluorouracil	Huang *et al.*, 2010
Chitosan + Nano-hydroxyapatite	Inorganic-organic hybrid materials for biomedical applications	Ruphuy *et al.*, 2016
Chitosan	Biocide as a replacement for pesticides	Alcântara, 2011
Chitosan + Tannins	Microspheres for pilot use in water treatment	Nakano, 2016

Given these considerations, the potential of CH is evidenced in various areas. In the biomedical sphere, chitosan is used extensively due to its ability to accelerate the healing process, antimicrobial activity, bioresorbability and coagulant effect (Felipe *et al.*, 2017).

2.5 Chondroitin sulphate

2.5.1 Glycosaminoglycans

Connective tissues comprise a viscous, semi-liquid and gelatinous fundamental substance composed mainly of carbohydrates known as mucopolysaccharides. GAGs polysaccharides (glycans) and amino sugars (glucosamine) are this substance's main types of carbohydrates. GAGs are linear and anionic heteropolysaccharides made up of repetitive disaccharide units of high molecular weight. They are polyanions capable of retaining a large amount of water. A fundamental characteristic of these disaccharide units is the presence of amino sugars, which can be N-acetylglucosamine or N-acetylgalactosamine, accompanied by other monosaccharides, such as uronic acids or galactose (Sanches, 2013).

The GAGs commonly found are CS, dermatan sulphate (DS), hyaluronic acid (HA), keratan sulphate (KS), heparin (HE) and heparan sulphate (HS) (Nakano *et al.*, 2010). CS is a linear anionic heteropolymer of D-glucuronic acid and N-acetyl-D-galactosamine, linked alternately by the β(1→3) and β(1→ 4) bonds, respectively. In addition, CS, shown in Figure 4, is a GAG present in the fundamental substance of vertebrate connective tissues, especially cartilage (Yu *et al.*, 2022; Santos, 2009).

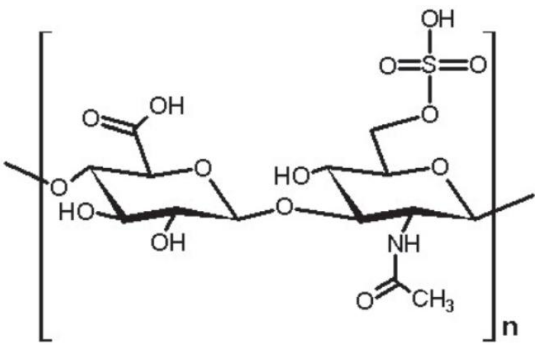

Figure 4 – Structure of the CS.

Adapted from Bunhack *et al.*, 2007.

CS synthesis begins with the production of the central protein inside the granular endoplasmic reticulum (GER) and its subsequent transportation to the Golgi complex. There, this process goes through three distinct stages: the formation of the binding region, the polymerisation (which involves the chains' elongation) and the polysaccharides' sulphation (Santos, 2009).

In terms of structure, this GAG can have different sulphation patterns, which can vary according to the cell type, tissue, organ, organism pathological conditions or age. However, CSs are always formed from alternate units of 4-linked β-D-glucuronic acid (GlcA) and N-acetyl-β-D-galactosamine (GalNAc), which is 3-linked and most often 4- and/or 6-sulphated. These monosaccharide units form the repetitive disaccharide unit of CS, as shown in Figure 5 (Pomin, 2013).

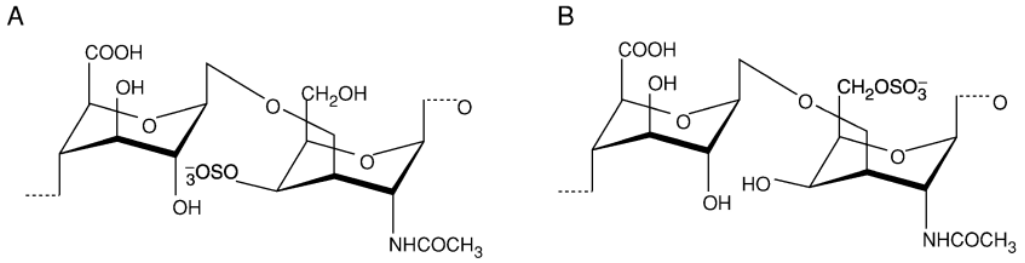

Figure 5 – Chemical structure of (a) chondroitin-4-sulphate and (b) chondroitin-6-sulphate.

Adapted from Pavão *et al.*, 2006.

2.5.2 Applications of CS

CS, combined with other compounds, can be applied in various areas, such as bone regeneration, dermal regeneration, food preservation, chondrogenesis and cancer cell treatment applications. A set of applications can be seen in Table 3.

Table 3 – Main forms and applications of CS-containing materials.

Compounds	Application	Reference
Chondroitin Sulphate + Chitosan	Nanoparticles for curcumin encapsulation	Jardim *et al.*, 2012
Chondroitin Sulphate + Chitosan	Microcapsules for proanthocyanidin encapsulation for food preservation	Yu *et al.*, 2022
Chondroitin Sulphate + Chitosan	Microcapsules for the controlled release of 5-fluorouracil	Huang *et al.*, 2010
Chondroitin Sulphate + Chitosan + Strontium	Scaffolds for bone reconstruction	Xu *et al.*, 2021
Chondroitin Sulphate + Chitosan	Scaffolds for use in prostate cancer cells	Xu *et al.*, 2020
Chondroitin Sulphate + Fibroin + Hyaluronic acid	Scaffolds for dermal tissue reconstruction	Yan *et al.*, 2013
Chondroitin Sulphate + Collagen + Gelatine + Hyaluronic acid	Scaffolds for stem cell chondrogenesis	Yang *et al.*, 2023

Studies carried out by Xu *et al.* (2020) showed that the developed CH-CS scaffolds may be an appropriate pre-clinical model for use as an in vitro prostate cancer platform for drug screening since changes in CS expression during the progression of prostate cancer suggest that it may serve as a possible marker for an unfavourable cancer prognosis. In addition, the work carried out by Yan *et al.* (2013) revealed that the prepared scaffolds offer great potential for dermal tissue regeneration, where CS accelerated cell metabolism, maintaining a typical environment for cell growth.

3 METHODOLOGIES

This work aims to produce scaffolds that simulate bone composition, i.e., the organic and inorganic parts of the bones. To this, the preparation and characterisation of the scaffolds were performed at the IPB and preliminary biological analyses, such as microbiological assay and in-vitro cell culture, were carried out at the UTFPR.

3.1 Materials

The materials used to carry out this work consist of aqueous HAp paste *nanoXIM-HAp102*, supplied by Fluidinova S.A., with a solids content of 15.0 ± 1.0% wt. and a particle size of <50 nm. The CH, 90/200/A1, purchased from Biolog-Biotechnologie GmbH (Germany), holds a degree of deacetylation and dynamic viscosity of 91.9% and 128 mPa·s, respectively. The CS was supplied by SM Empreendimentos Farmacêuticos LTDA (Brazil). The CH solution was prepared using acetic acid glacial, purchased from Fisher Chemical. To maintain the pH of the dispersion at 5.5, an acetate buffer was prepared from 1M acetic acid solution and 1M sodium hydroxide (NaOH) solution.

3.2 Preparation of the dispersions

The dispersions were prepared following the methodology proposed by Ruphuy *et al.* (2016), with some modifications. To prepare the base scaffolds (HAp/CH 70/30), a solution of 3% (w/v) CH (in 1% m/v acetic acid solution) and the aqueous HAp paste were used. As shown in the scheme of Figure 6 (Ruphuy *et al*., 2016), after adding the CH solution volume (~28.8 mL) with ~57.7 mL of acetate buffer (pH 5.5), the HAp paste (~13.5 mL) was injected using a peristaltic pump at 240 rpm, while the solution was stirred by an Ultra-Turrax (a high-speed dispersion homogeniser device (Miccra D-9) at its minimum speed (11 000 rpm) for 2 minutes. The addition of CS was tested at different concentrations, following different strategies. The needed amount of CS was weighed and added to the CH solution.

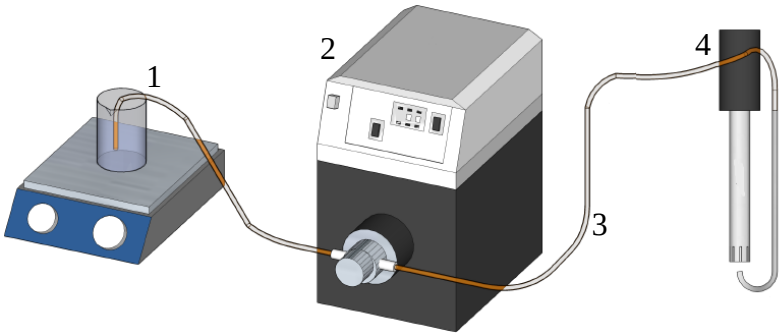

Figure 6 – Experimental scheme used to prepare the dispersions: (1) beaker under agitation; (2) peristaltic pump; (3) tube; (4) Ultra-Turrax.

Adapted from Ruphuy *et al.*, 2016.

3.3 Scaffold preparation

A methodology adapted from the one proposed by Ruphuy *et al.* (2016) was followed to prepare the scaffolds. To this, 10 mL of the dispersions were placed in polystyrene Petri dishes with a diameter of around 55 mm and stored in a freezer for 24 hours. The samples were then freeze-dried and stored appropriately in plastic bags until characterisation.

3.4 Scaffolds purification

Following the methodology described by Ruphuy *et al.* (2016) and Ruphuy *et al.* (2018), the scaffolds were purified using supercritical CO_2 treatment ($scCO_2$), as shown in Figure 7. The reason for choosing this treatment is linked to its benefits: it is non-toxic, environmentally benign, non-flammable and non-corrosive technique (Ruphuy *et al.*, 2018).

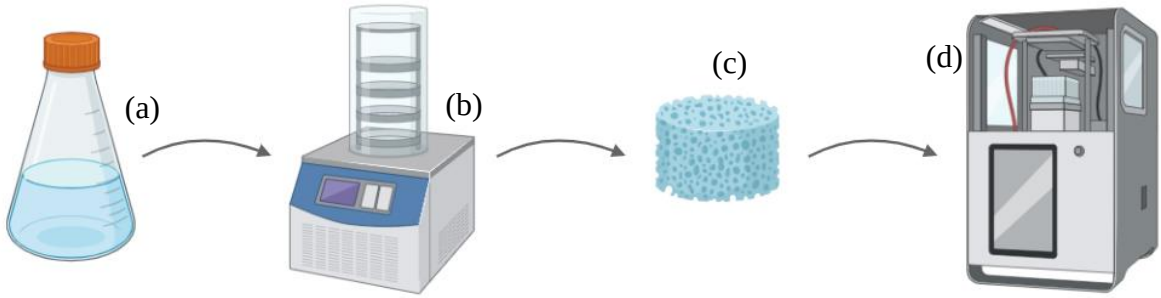

Figure 7 – Schematic representation of scaffold purification: (a) dispersion; (b) freeze drying; (c) scaffold; (d) acetic acid extraction with $scCO_2$.

Adapted from Ruphuy *et al.*, 2018.

Despite its many advantages, the $scCO_2$ extraction method is expensive to install, requires the application of high pressure and has limitations on the materials subjected to this purification process (White *et al.*, 2021; Manjare & Dhingra 2019).

In the purification process, the samples were distributed equally inside a 1 L extraction cell. CO_2 from a standard cylinder was cooled, pumped into the cell and compressed to a constant pressure of 8.0 MPa. The temperature was increased to reach the supercritical state, with experiments carried out in static mode for 5 samples per experiment. The temperature of 75°C was selected, in line with Ruphuy *et al.* (2018), who reported 80% removal of residual acetic acid under these conditions (75°C and 8.0 MPa). After each cycle, two depressurisation steps were carried out: the first at 4 MPa and the second at 0.2 MPa (Ruphuy *et al.*, 2016; Ruphuy *et al.*, 2018).

3.5 Scaffolds characterisation

The scaffold samples were characterised concerning density to examine the scaffold's structure, composition, and porosity, as well as aspects that favour cell adhesion, migration, and organisation. This was done to ensure biocompatibility and safe interaction with the organism. The scaffolds' biological properties were evaluated to investigate how the cells responded to them, including viability, cytotoxicity and cell proliferation.

3.5.1 Fourier transform infrared spectroscopy (FTIR)

FTIR analysis was conducted using a Fourier transform infrared spectrophotometer, model MB3000 from ABB Inc. (Quebec, Canada), operating in ATR mode. The spectra were acquired from 4000 to 550 cm^{-1}, averaging 32 scans min^{-1} at a resolution of 4 cm^{-1}, using the Horizon MB v.3.4 software (Schreiner *et al.*, 2021; Ruphuy *et al.*, 2016).

3.5.2 Scanning electron microscopy (SEM)

SEM analysis was carried out using a Phenom Pro microscope from Phenom-World (Eindhoven, Netherlands) to obtain information on the morphological properties of the scaffolds. The samples were placed in carbon sheet pins and analysed at 15 kV.

3.5.3 Thermogravimetric analysis (TG)

The thermal stability of the scaffolds was analysed using NETZSCH equipment (TG 209 F3 Tarsus, Selb, Germany). The samples were heated from 30° to 700°C at 10 °C/min under an inert atmosphere (nitrogen) with a 50 mL/min flow rate (Crugeira *et al.*, 2023). The peak related to acetic acid degradation was analysed, and each sample's residual amount of acetic acid was estimated from this mass loss by comparing the treated ($scCO_2$) and untreated samples. The extraction yield was calculated by comparing the acetic acid content in each sample with that of a sample that had not undergone any purification or neutralisation process (Ruphuy *et al.*, 2018).

Equation 1 was used to obtain the extraction yield value. Where AAC_{scCO_2} represents the acetic acid content obtained by the samples that underwent the $scCO_2$ treatment and $AAC_{untreated}$ for the samples that did not underwent the treatment.

$$Extraction\ yield = 100 - \left(\frac{AAC_{scCO_2} \times 100}{AAC_{untreated}}\right) \quad (1)$$

3.5.4 Density

The density was determined experimentally by measuring the height and diameter with a calliper and the weight with an analytical balance in triplicate (Ruphuy *et al.*, 2018).

3.5.5 Swelling test

Swelling tests were carried out to analyse the swelling capacity (C_w), i.e., the ability of the scaffold to absorb water. To this, the samples were weighed after drying (W_d) and swollen (W_s) after being immersed in a PBS solution (pH of 7.4). C_w was calculated according to Equation 2. The immersion times vary from 0 to 60 minutes (Ruphuy *et al.*, 2018).

$$C_w(g/g) = \frac{W_s - W_d}{W_d} \quad (2)$$

3.5.6 Cytotoxicity assay

Carrying out biological tests on scaffolds is essential to guarantee safety and efficacy in clinical applications since these tests allow the creation of environments that mimic the natural cellular microenvironment. To this end, cytotoxicity was analysed using the methylthiazolydiphenyl-tetrazolium bromide (MTT) assay (3-[4,5-dimethylthiazol-2-yl]-2,5-diphenyltetrazolium bromide). This analysis makes it possible to check whether the materials harm cell health.

The selection of the cell type is fundamental, since fibroblasts, which belong to connective tissue (Plikus *et al.*, 2021), and bone cells, which are components of both bone and connective tissue (Bahraminasab *et al.*, 2021), exhibit different metabolic and behavioural responses in the MTT assay.

For this purpose, the analysis was carried out according to the protocol suggested by Mosmann (1983) with the necessary adaptations for evaluating scaffolds based on the work of Mohammadi *et al*. (2024).

The scaffolds, with a diameter of 7 cm and an average mass of 2.8 mg, were placed at the bottom of 24-well plates. A suspension of 2×10^4 NIH3T3 or MG63/cm^2 cells, diluted in DMEM culture medium and supplemented with 10% fetal bovine serum, was placed on them. The negative control group (CO-) contained only cells and supplemented culture medium. The positive control group (CO+) contained cells and the cytotoxic agent methyl methanesulphonate (MMS - 150 µM diluted in supplemented culture medium).

The plates were then incubated for 24 and 48 hours. After this process, the medium was removed with serum and replaced with culture medium containing MTT (0.167 mg/mL). The plates were incubated for another four hours, and the medium with MTT

was replaced with 100 µL of dimethylsulphoxide (DMSO) to solubilise the formazan crystals. The absorbance was read on a microplate reader (Thermo Plate) at 492 nm.

The percentage values of cell viability (CV) were estimated by the ratio between the absorbance of the treatment and the absorbance of the negative control, according to Equation 3.

$$CV = \left(\frac{ABS_T}{ABS_{C0-}}\right) \times 100 \quad (3)$$

Where CV is the cell viability (%), ABS_T is the absorbance of the treatment, and ABS_{C0-} is the absorbance of the negative control.

The absorbance values were subjected to the normality test, analysis of variance (one-way ANOVA) and Dunnet's mean comparison test (α = 0.05), using *Action Stat* software.

3.5.6.1 Cell culture

NIH3T3 cells, fibroblasts derived from *Mus musculus* embryonic tissue, and MG63 cells (Figure 8), derived from human bone tissue, were grown in 25 cm^2 culture flasks containing 10 mL of DMEM (Dulbecco's Modified Eagle Medium) culture medium, supplemented with 15% fetal bovine serum, and incubated in an incubator at 37 °C with 5% CO_2. The cells were obtained from the Rio de Janeiro Cell Bank.

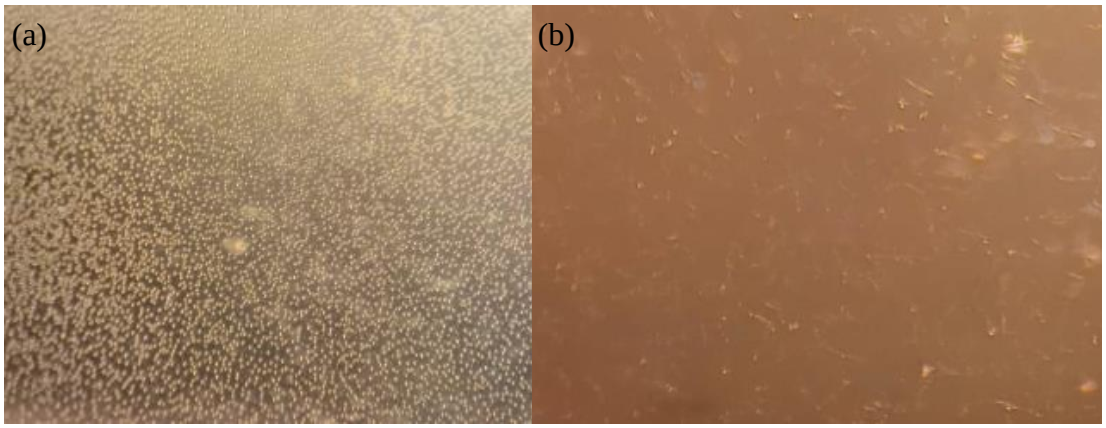

Figure 8 – Stereoscopic microscope image of (a) NIH3T3 and (b) MG63 cells.

4 RESULTS AND DISCUSSION

4.1 Scaffold preparation

4.1.1 Preliminary results

As initial tests, different HAp, CH and CS concentrations were trialled to produce the scaffolds. Trials were carried out using the ratios HAp:CH:CS of 70:25:5, 70:0:30 and 69:30:1. The scaffolds maintained the inorganic/organic ratio of 70/30 ratio and were produced according to the methodology defined by Ruphuy *et al*. (2016), as previously described in the experimental section. The CH was directly replaced with the CS in the first two assays (70:25:5, 70:0:30). In the third assay, 1% of CS was added, maintaining the total solids content in the dispersion. Figure 9 shows the three formulations produced and the blank formulation (70:30:0).

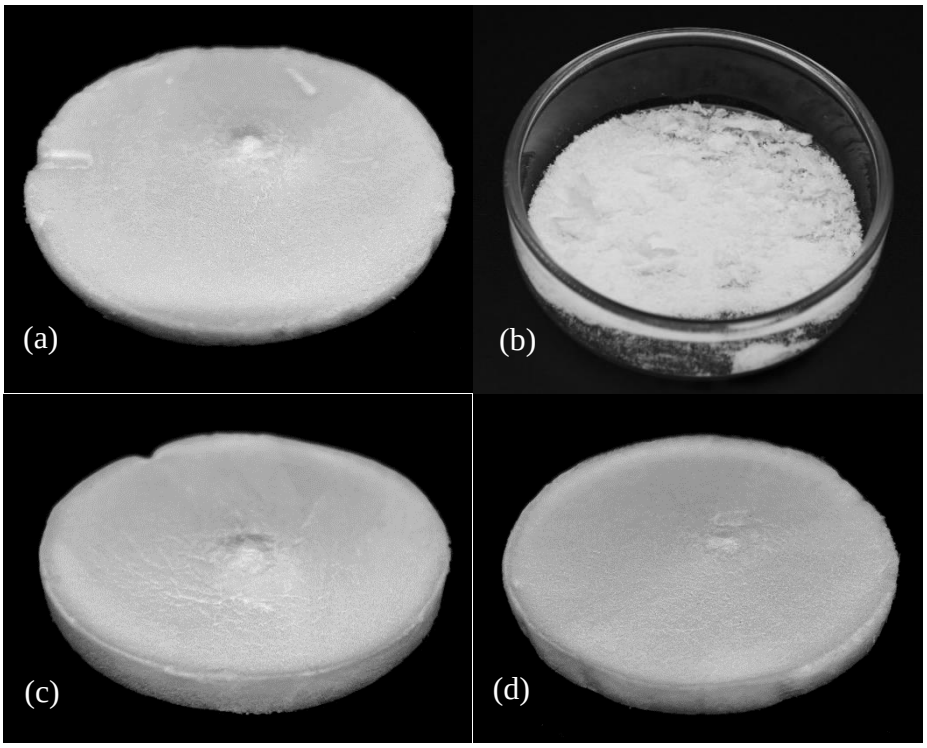

Figure 9 – Preliminary tests with the formulations (a) 70:25:5, (b) 70:0:30, (c) 69:30:1 and (d) 70:30:0.

In the 70:25:5 scaffolds, the 30% of the organic phase comprised 25% of CH and 5% of the CS, keeping the total solids concentration constant. After the freeze-drying process, the scaffolds preserved their disc-shaped structure but became brittle. When all the CH was replaced by CS, i.e., the 70:0:30 formulation, the disc structure was not maintained, and the scaffolds were turned into powder after freeze-drying. According to these results, it is perceptible that the CH component helps maintain the structural support

and flexibility of the scaffold (Fourie *et al*., 2022). CS alone was insufficient to provide the necessary structural stability, being more effective when combined with other materials that contribute to mechanical integrity, such as CH (Fernandes, 2009). The interaction between these two polymers, with CH acting as a cationic polymer and CS as an anionic polymer, results in structures with higher resistance to mechanical stress and better performance under stress conditions such as pH changes and humidity (Alinejad *et al*., 2018). Another essential reason for keeping CH in the scaffold formulation is that CH is degraded in vivo mainly through enzymatic hydrolysis, a desirable characteristic as the material should break down and be reabsorbed after tissue formation, maintaining mechanical strength similar to that of the original tissue up to that point (Kakazu & Malmonge, 2014).

For the 69:30:1 formulation, 1% CS was added to the total mass of the HAp plus CH, but the total solids content was maintained. The sample preserved its disc shape in this case and did not become brittle. This result may be related to the fact that the ratio HAp/CH was kept constant, ensuring that both CH and HAp continued to provide the necessary structural support for the scaffold. For this reason, it was decided to manufacture the scaffolds maintaining the 70:30 HAp:CH ratio. In the first case (Case A), CS was added directly to the base formulation/scaffold (formulation without CS), increasing the total solids content of the formulation as the CS content increased. In the second case, the total solids content was maintained (Case B). Concerning the characterisation, the 70:0:30 sample was not analysed, as it did not retain its disc-shaped structure.

4.1.2 Scaffolds prepared according to Case A formulations

To prepare the scaffolds according to Case A, to the base formulation where a fixed amount of HAp paste and CH were used, CS was added at concentrations of 1%, 2.5% and 5%. The samples were labelled as A.1%, A.2.5% and A.5%, respectively. The visual aspect of the samples is shown in Figure 10. The masses used to prepare the respective samples are shown in Table A.1 provided in Appendix A.

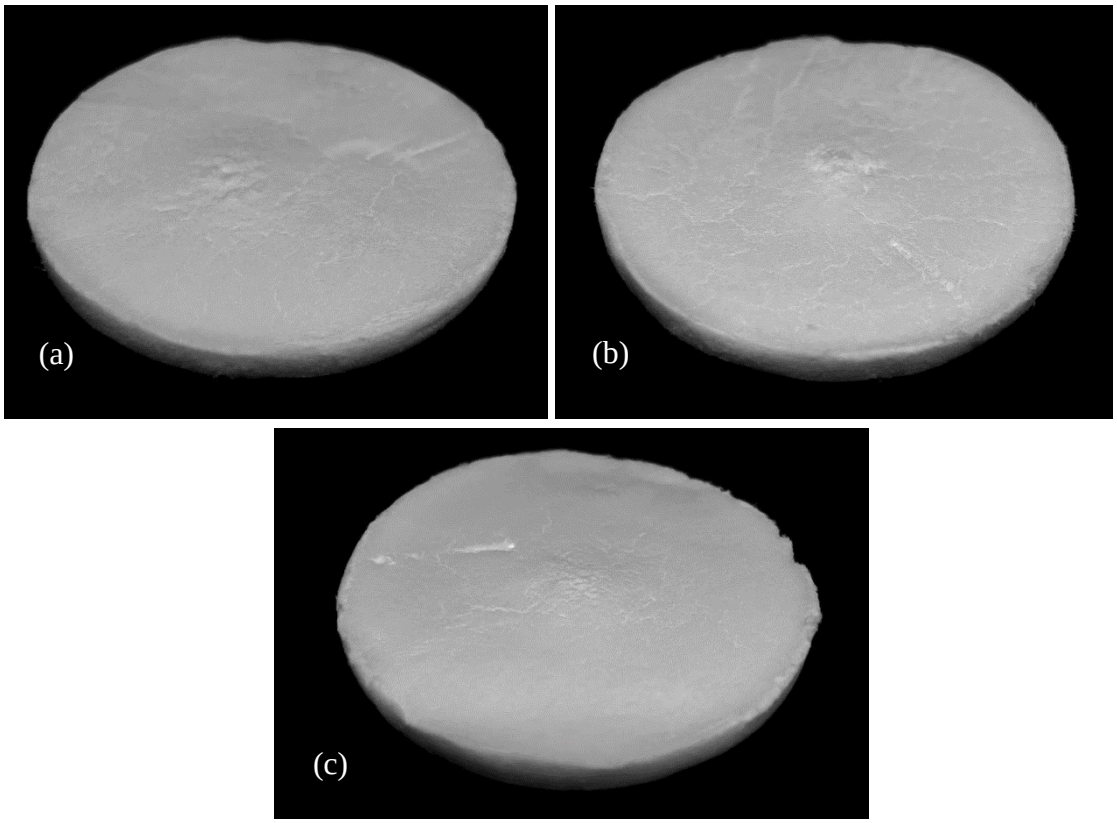

Figure 10 – Formulation Case A (a) A.1%, (b) A.2.5% and (c) A.5%.

In this case, it was observed that the samples remained disc-shaped, independent of the used CS content, with the sample A.5% presenting a brittle appearance. Samples A.1% and A.2.5% did not become brittle and had a good structural aspect.

4.1.3 Scaffolds prepared according to Case B formulations

To prepare the scaffolds according to Case B, and to keep the total solids constant, the mass of HAp and CH were proportionally reduced according to the added CS and in order to keep the HAp:CH at 70:30. The CS content varied from 1%, 2.5% and 5% with the respective samples labelled as B.1%, B.2.5% and B.5%. The visual aspect of the scaffolds produced in Case B are presented in Figure 11. The masses used to prepare the respective samples are shown in Table A.1 provided in Appendix A.

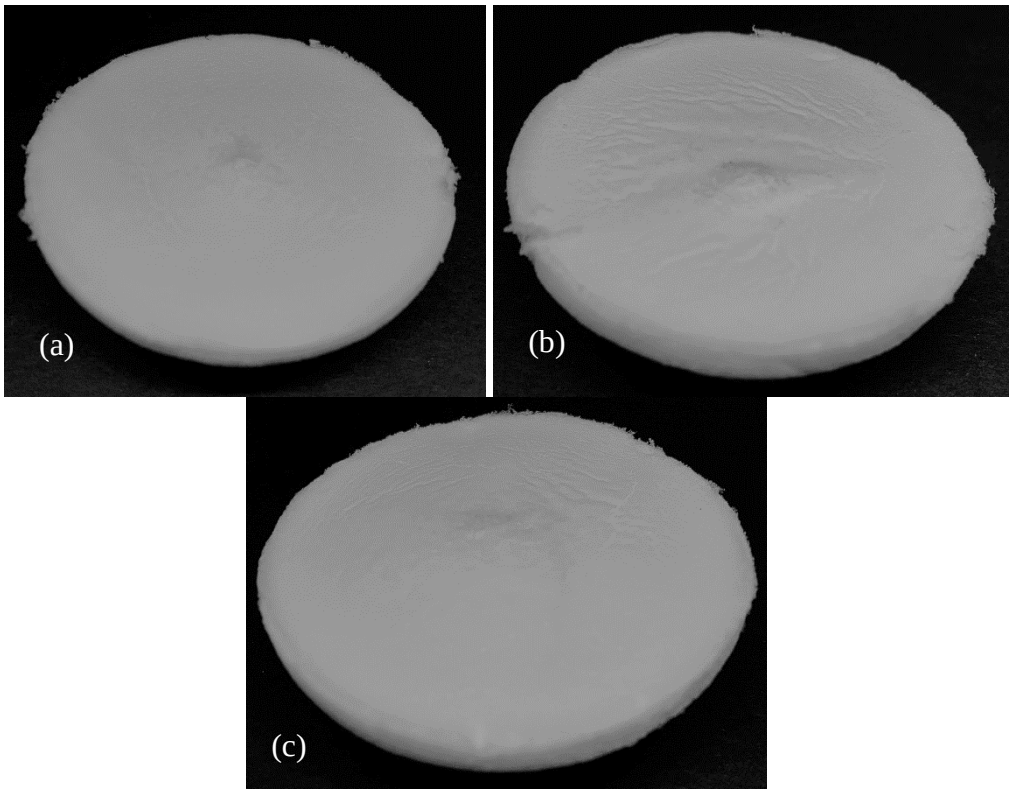

Figure 11 – Formulation Case B (a) B.1%, (b) B.2.5%, and (c) B.5%.

All the samples retained their disc shape. However, as in Case A, sample B.5% also becomes brittle. Samples B.1% and B.2.5% maintained good structural integrity. Visually, there were no visual or structural differences between the samples from Cases A and B.

4.2 Scaffold characterisation

4.2.1 Fourier transform infrared spectroscopy (FTIR)

FTIR analysis is essential in characterising scaffolds, as it identifies functional groups and chemical bonds, providing information on molecular composition and structural changes. This ensures that the material has the suitable chemical properties to interact with the biological environment, as well as helping to verify biocompatibility and stability, which are fundamental for efficient and safe tissue regeneration.

The FTIR spectra of the samples (preliminary samples and samples of Case A and Case B), are shown in Figure 12, where the most representative bands are assigned. For comparison purposes each image presents the untreated and treated ($scCO_2$) samples.

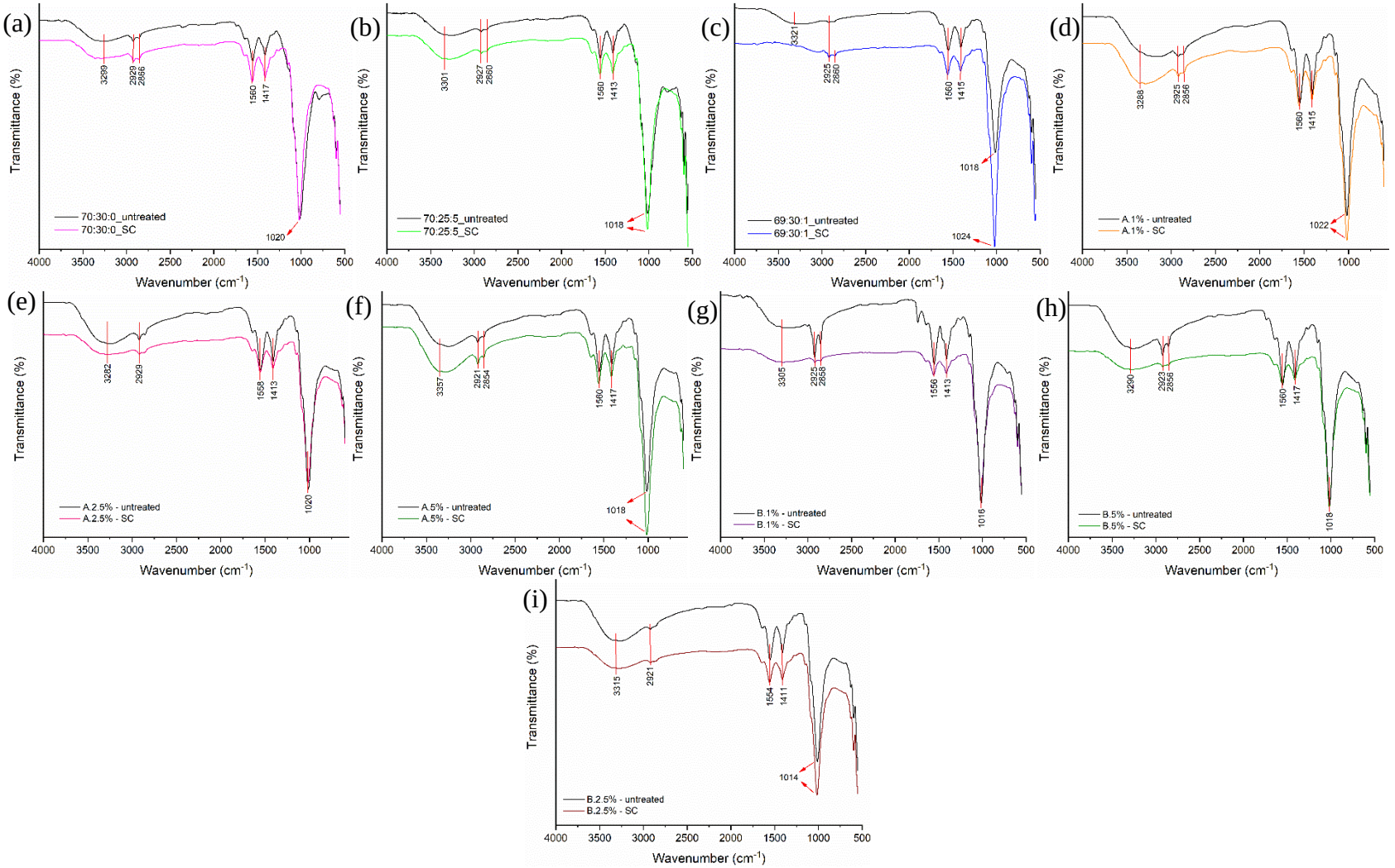

Figure 12 – FTIR spectrum for samples (a) 70:30:0, (b) 70:25:5, (c) 69:30:1, (d) A.1%, (e) A.2.5%, (f) A.5%, (g) B.1%, (h) B.2.5% and (i) B.5%.

The peaks in the 3290-3321 cm^{-1} range are characteristic of the hydroxyl group (-OH), while the peaks in the 2921-2860 cm^{-1} range are due to the -C-H group. The peak at 1550-1560 cm^{-1}, represents the deformation vibration of the -N-H group. The peaks at 1417-1411 cm^{-1} can be associated with a combination of CN-NH, CH_2-OH and CH_3 bands. The typical bands of the phosphate group (PO_4), are translated in the peaks at 1024-1014 cm^{-1}, corresponding to the triple degenerate asymmetric stretching vibration of the phosphate P-O bond (Ruphuy *et al*., 2016; Xu *et al*., 2021; Basik & Mobin, 2020; Fadeeva *et al*., 2011).

The samples that underwent the $scCO_2$ treatment showed increased peaks at 1024-1014 cm^{-1}. This may indicate that undergoing the treatment, i.e., being exposed to high temperature and pressure conditions, increased the sample's crystallinity rate, which resulted in the intensification of the peaks, as mentioned earlier (Ewing & Kazarian, 2018). This phenomenon occurs because crystalline regions have less structural disorder, allowing molecular vibrations to occur in a more homogeneous environment, generating a sharper and more defined spectral signal.

4.2.2 Scanning electron microscopy (SEM)

SEM analysis makes it possible to observe the morphology of the scaffold in high resolution, including the size, shape and distribution of the pores, as well as assess the interconnectivity of these pores, which are essential factors in ensuring cell adhesion, proliferation and nutrient flow. This analysis also allows the detection of possible structural defects and irregularities that could compromise the mechanical integrity and effectiveness of the scaffold.

Figure 13 shows the images obtained from the SEM analysis of Cases A and B (treated samples). The ones corresponding to the preliminary tests were not analysed. It is possible to observe differences in the formulations, as the samples from the two cases have different characteristics.

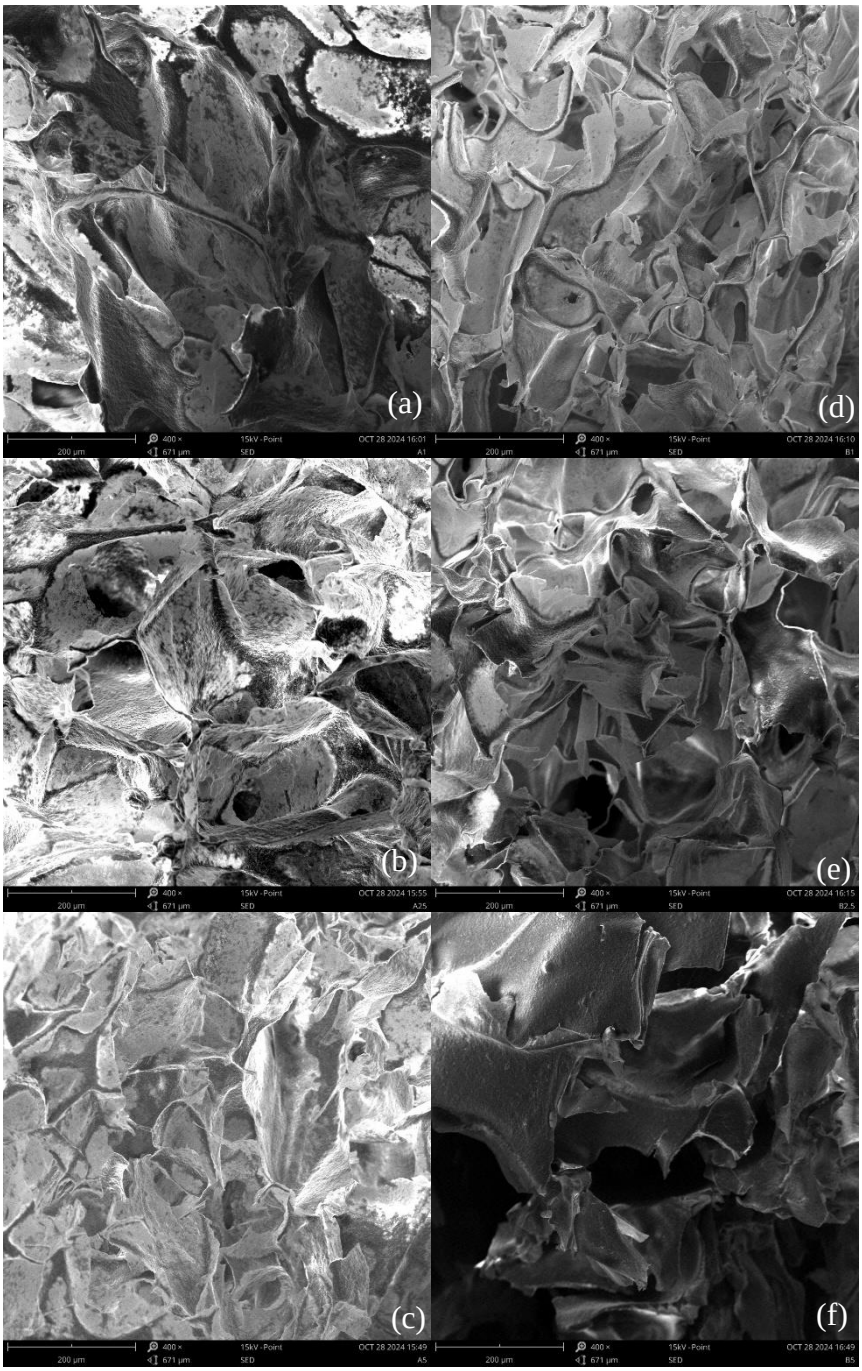

Figure 13 – SEM micrographs of a cross-section of (a) A.1%, (b) A.2.5%, (c) A.5%, (d) B.1%, (e) B.2.5%, and (f) B.5%.

The porosity of scaffolds is fundamental for supporting cell growth, proliferation and migration, facilitating the diffusion of nutrients and improving their mechanical properties (Teixeira, 2016; Cordeiro, 2019). The images show that these scaffolds have low porosity, which increases mechanical strength and structural stability, advantageous for applications that demand high durability, such as bone tissue. However, this low porosity can limit cell proliferation and hinder vascularisation and nutrient diffusion, impairing cell viability in the inner layers (O'Brien, 2011).

4.2.3 Thermogravimetric analysis (TG)

Figure 14 shows the thermograms obtained from the TG analysis of the $scCO_2$-treated and untreated samples (samples of the preliminary tests and samples of Case A). The samples corresponding to the Case B are not presented due to problems with the used equipment.

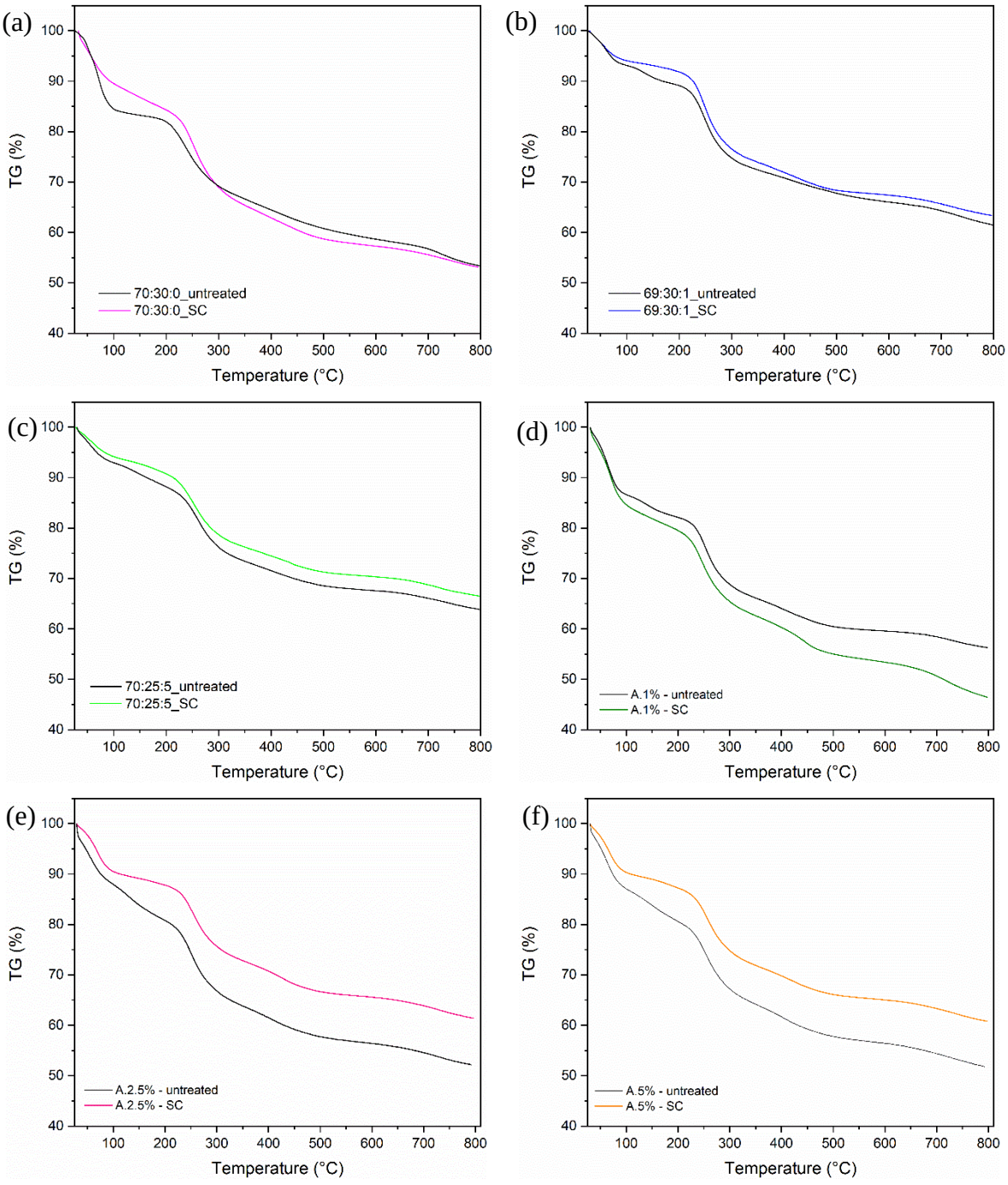

Figure 14 – TG for samples (a) 70:30:0, (b) 69:30:1, (c) 70:25:5, (d) A.1%, (e) A.2.5%, and (f) A.5%.

It can be seen that the first mass loss, from 30-100 °C, is related to the evaporation of water (Xu *et al*., 2021). In the 100-195 °C range, the observed mass loss is related to the degradation of the acetic acid present in the sample (Ruphuy *et al*., 2018). Above 200 °C, the mass loss refers to the degradation of the CH present in the sample composition, since the degradation of polysaccharides occurs in this temperature range (Georgieva *et al*., 2012). The percentage of residual sample is attributed to the amount of HAp used in the formulations, which varied between 60% and 70%. As expected, the residual percentage also remained in this range, reflecting the amount of HAp incorporated into each formulation (Ruphuy *et al*., 2018). The complete degradation stages and corresponding mass loss are presented in Table A.2 in Appendix A. The mass loss for the samples from the preliminary tests and Case A were calculated on a water-free basis.

It is also possible to note that, unlike the preliminary samples, the Case A samples showed a fourth degradation peak, located between 390 and 450 °C, which represents the degradation of CS (Oliveira *et al*., 2017), indicating a mass loss of approximately 6%.

Tables 4 and 5 show the residual acetic acid data obtained from the degradation peak and the treatment efficiency for preliminary tests and Case A, respectively.

Table 4 – Residual acetic acid data and treatment efficiency for preliminary tests.

Sample		Acetic acid content (wt. %)	Extraction yield (%)
Untreated	70.30.0	2.08	-
	75.25.5	4.53	-
	69.30.1	3.6	-
Supercritical CO_2 treatment	70.30.0	0	100
	75.25.5	1.93	57
	69.30.1	0	100

Table 5 – Residual acetic acid data and treatment efficiency for Case A.

Sample		Acetic acid content (wt. %)	Extraction yield (%)
Untreated	A.1%	4.12	-
	A.2.5%	6.64	-
	A.5%	6.09	-
Supercritical CO_2 treatment	A.1%	0	100
	A.2.5%	1.84	72
	A.5%	2.71	56

Regarding the residual acetic acid, it can be seen that the samples that did not undergo the $scCO_2$ treatment have a higher content, between 4 and 6%. The value of samples that have undergone treatment is zero or between 1 and 3%. This shows that the $scCO_2$ treatment effectively removes acetic acid, with samples reaching extraction yields between 55 and 80%, or even 100% in particular cases. The results obtained by Ruphuy *et al.* (2018) under the same conditions were 4.1% for the untreated sample and 0.8% for the treated sample, corresponding to an extraction yield of 80%. It is also perceived from the obtained results that CS seems to make acetic acid extraction difficult since high residual acetic acid values were obtained for these samples after applying supercritical treatment. The presence of acetic acid can impart cytotoxicity to the final materials and make their use problematic for cell growth.

4.2.4 Density determination

Table 6 shows the results obtained for the scaffold density analysis. It can be seen that the values obtained are consistent with those of Chan (2016), who recorded a density of 0.0423 ± 0.0028 for a 70/30 HAp/CH scaffold composition prepared under similar conditions. The results obtained in the work carried out by Szustakiewicz *et al*. (2021), where scaffolds were made from HAp and poly(L-lactide) (PLLA), the density values found for the samples ranged from 0.030 ± 0.002 to 0.037 ± 0.005, showing that they are close to the values found for this work.

It can also be seen that the addition of CS did not significantly modify the density of the samples compared to the control sample (0.0464 ± 0.0037).

Table 6 – Results obtained from density analysis.

Samples	Density (g/cm^3)
70:30:0	0.0464 ± 0.0037
70:25:5	0.0495 ± 0.0028
69:30:1	0.0436 ± 0.0013
A.1%	0.0488 ± 0.0004
A.2.5%	0.0494 ± 0.0086
A.5%	0.0499 ± 0.0032
B.1%	0.0578 ± 0.0060
B.2.5%	0.0510 ± 0.0096
B.5%	0.0521 ± 0.0030

In general, scaffolds have low densities due to porosity, which is crucial for functionality in tissue engineering applications. This ensures a balance between rigidity and biological integration capacity since introducing pores reduces density, facilitating nutrient exchange and cell colonisation (Farazin & Ghasemi, 2022; Gritsch *et al*., 2019).

4.2.5 Swelling tests

The importance of carrying out swelling tests is directly related to the application of the scaffold, as the swelling test simulates the conditions of a physiological environment. These tests are relevant because porosity and fluid absorption by the scaffold are essential for promoting the diffusion of nutrients, facilitating the removal of waste and, above all, guaranteeing a favourable environment for cell proliferation and differentiation. In addition, swelling behaviour directly influences the biocompatibility, structural integrity and functionality of the implanted material, since this analysis makes it possible to assess the material's ability to absorb liquids and expand.

In order to avoid sample degradation, and based on the previous studies of Ruphuy *et al*. (2018), the test was only carried out on samples that had undergone $scCO_2$ treatment. With this in mind, the swelling test was carried out in PBS medium (pH 7.4) for all the samples The tested time interval was between 0 to 60 minutes. The result of the analysis can be seen in Figure 15 for the 3 studied series (preliminary tests, Case A and Case B tests).

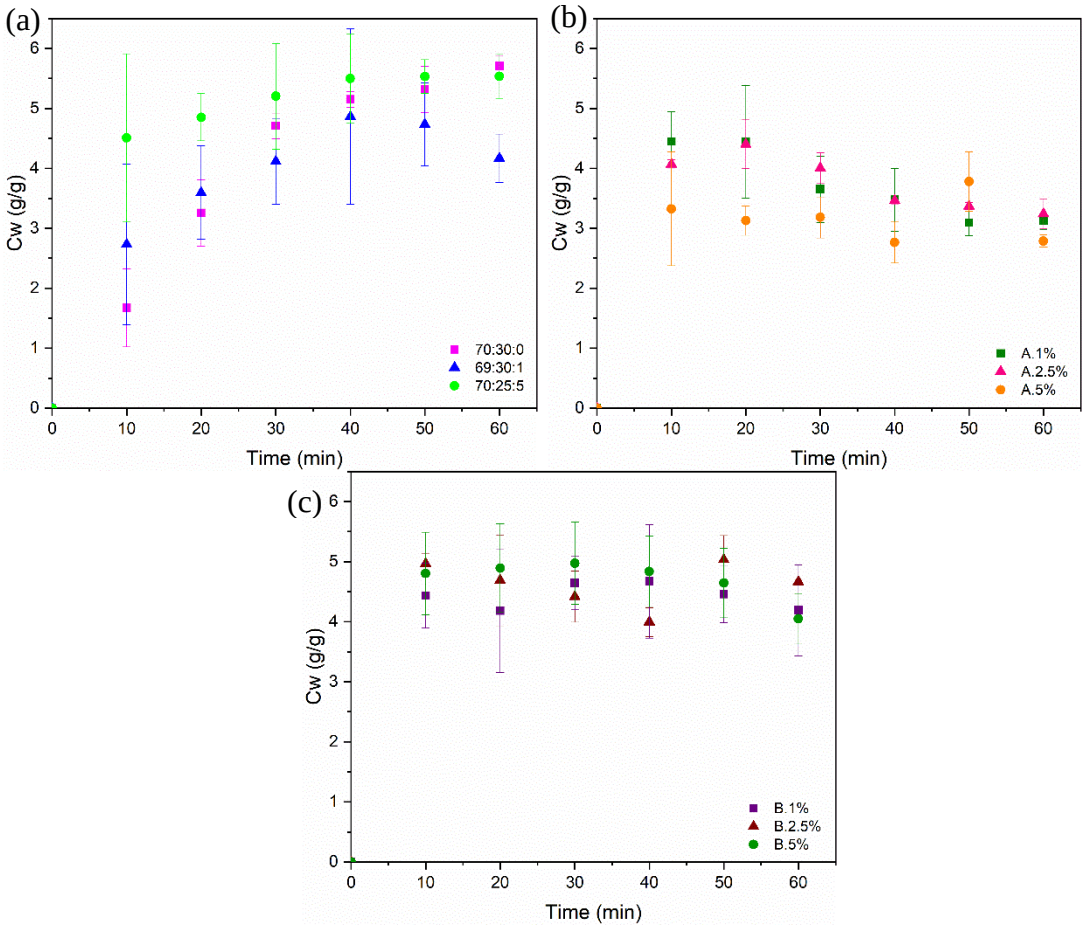

Figure 15 – Swelling test for the produced samples (a) preliminary tests, (b) Case A and (c) Case B.

It can be seen that the scaffolds began to swell within the first 10 minutes of analysis, and from that point there was no significant variation in the absorption capacity of the samples. Furthermore, it can be seen that the sample containing 5% CS, both the ones corresponding to Case B and the preliminary tests, showed the best curve for C_w, remaining stable after 10 minutes of analysis. This shows that there was no significant change in the swelling of the sample over the 60 minutes of analysis. Although HAp is not soluble in water (Cunha, 2010), the high C_w observed can be associated with the hydrophilic nature of the CH and CS present in the samples (Xu *et al.*, 2021).

Based on the observed behaviour, it can be concluded that the presence of CS did not significantly impact the absorption capacity. The values obtained for the samples (60 min) with CS are presented in Table 7.

Table 7 – C_w obtained for all samples after 60 minutes of analysis.

Samples	C_w (g/g)
70.30.0	5.71±0.17
70.25.5	5.53±038
69.30.1	4.17±0.41
A.1%	3.12±0.14
A.2.5%	3.24±0.24
A.5%	2.79±0.10
B.1%	4.19±0.76
B.2.5%	4.67±0.02
B.5%	4.05±0.42

This analysis indicates that the Case B samples were close to the control sample after 60 minutes. The B.5% sample proved to be the most effective in terms of swelling control, with a consistent curve and uniform C_w values at the registered 10-minute intervals. This uniformity suggests that the B.5% sample has properties that help stabilise the swelling process, resulting in minimal dispersion of the values, which is also consistent with a more resistant material.

These variations are not so discrepant and are in line with the literature, as reported by Xu *et al*. (2021), in which scaffolds composed of CH, CS and strontium had C_w values of 8.67 ± 6.6 g/g, 8.50 ± 0.7 g/g and 6.54 ± 0.21 g/g. In comparison, the study by Chan (2016), which produced scaffolds containing HAp and CH, obtained a swelling capacity of 24.5 ± 2.7 g/g, much higher than the values achieved with the materials developed in the present work.

4.2.6 Cytotoxicity assay

The samples that were subjected to the cytotoxicity analyses were the samples produced in the preliminary tests (70:25:5, 69:30:1, and 70:30:0), as these were the only ones sent to UTFPR so far, where the test was carried out. Figure 16 shows MG63 cells exposed to the treatments, and Figure 17 shows the NIH3T3 and MG63 cells with diluted formazan crystals after the MTT assay.

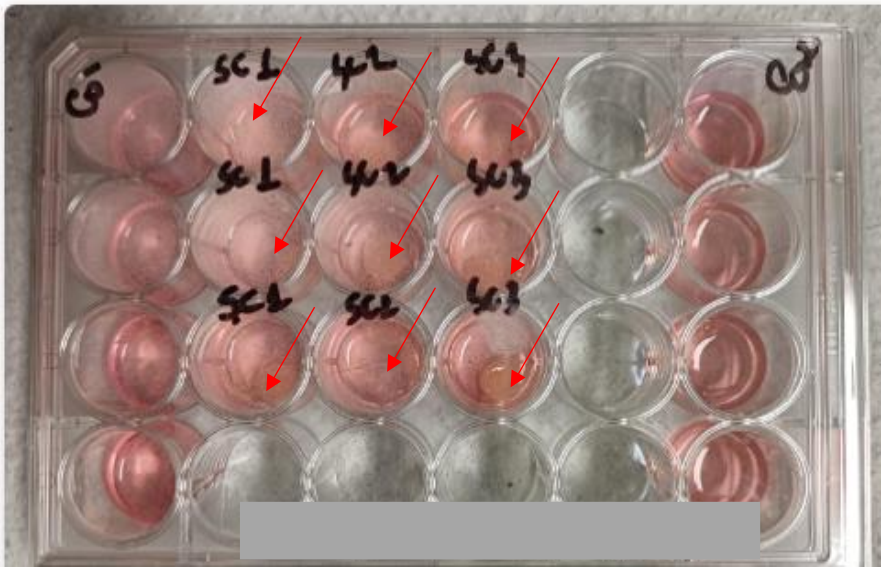

Figure 16 – MG63 cells exposed to the treatments.

Red arrows indicate the presence of the scaffolds in the wells.

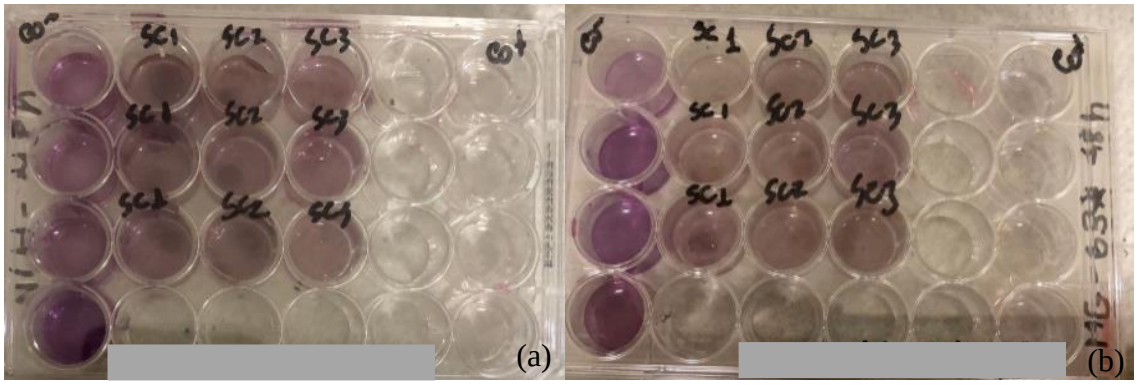

Figure 17 – Plate of (a) NIH3T3 and (b) MG63 cells with diluted formazan crystals.

The results of the MTT cytotoxicity test on NIH3T3 fibroblast cells (Figure 18) and MG63 bone cells (Figure 19) exposed to the scaffolds show that none of the evaluated samples were cytotoxic to these cell lines, as they had mean absorbances similar to those of the negative control and cell viabilities (Table 8) above 74.01%. Furthermore, it is possible to observe fibroblast cells (Figure 20) and bone cells (Figure 21) growing in the presence of the scaffolds.

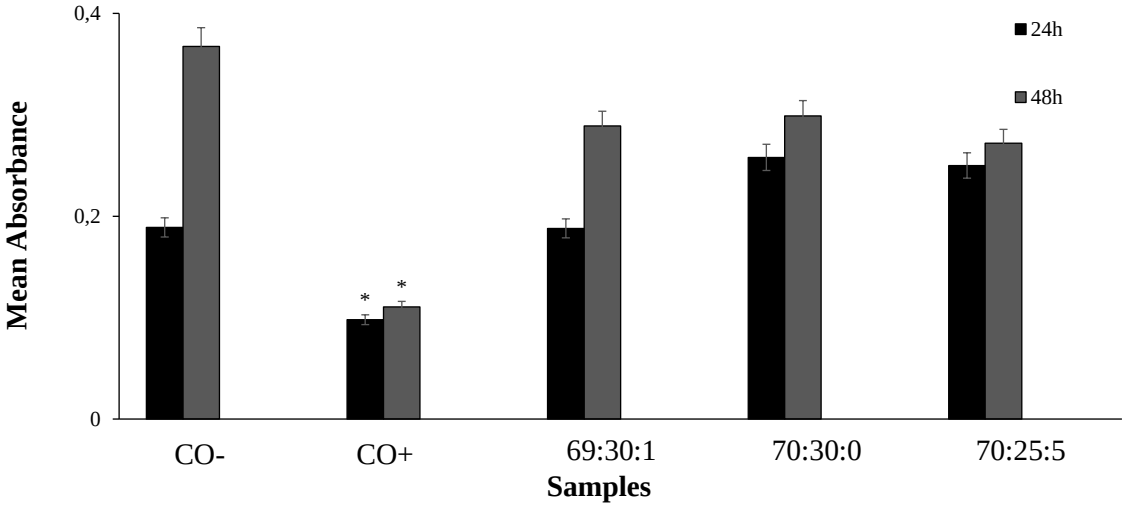

Figure 18 – Mean absorbance and standard deviation of NIH3T3 cells treated for 24 and 48 hours obtained for the scaffolds.

CO-: Negative Control; CO+: Positive Control.

* Results statistically different from the negative control (Dunnet's test, $p<0.05$).

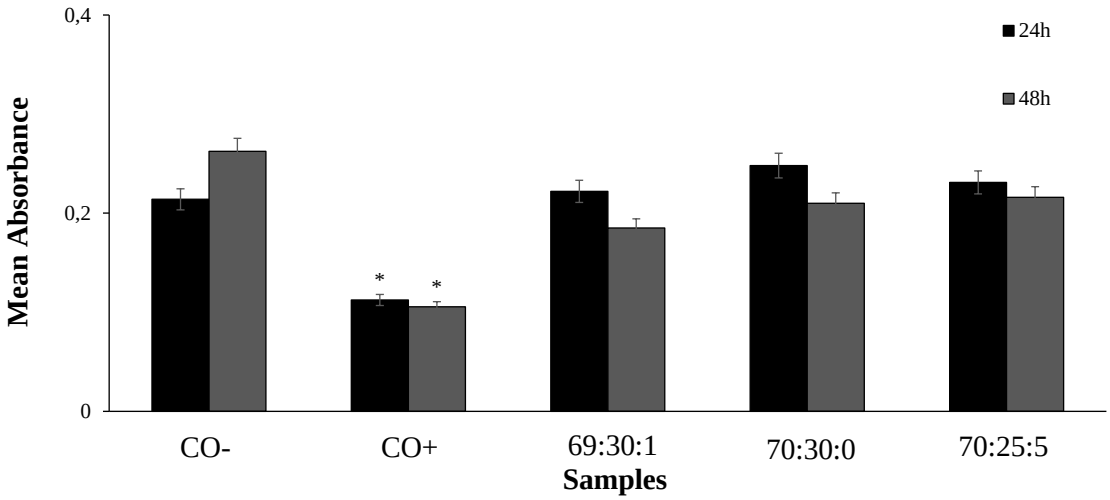

Figure 19 – Mean absorbance and standard deviation of MG63 cells treated for 24 and 48 hours obtained for the tested scaffolds.

CO-: Negative Control; CO+: Positive Control.

* Results statistically different from the negative control (Dunnet's test, $p<0.05$).

Table 8 – Percent cell viability (CV) of NIH3T3 and MG63 cells treated for 24 and 48 hours with the scaffolds, using the MTT test.

Samples	CV [%]			
	NIH3T3		MG63	
	24h	48h	24h	48h
CO-	100.00	100.00	100.0	100.0
CO+	51.85	30.07	52.57	40.19
69:30:1	99.47	78.64	103.74	70.48
70:30:0	136.51	81.36	115.89	80.00
70:25:5	132.28	74.01	107.94	82.29

CO-: Negative Control; CO+: Positive Control.

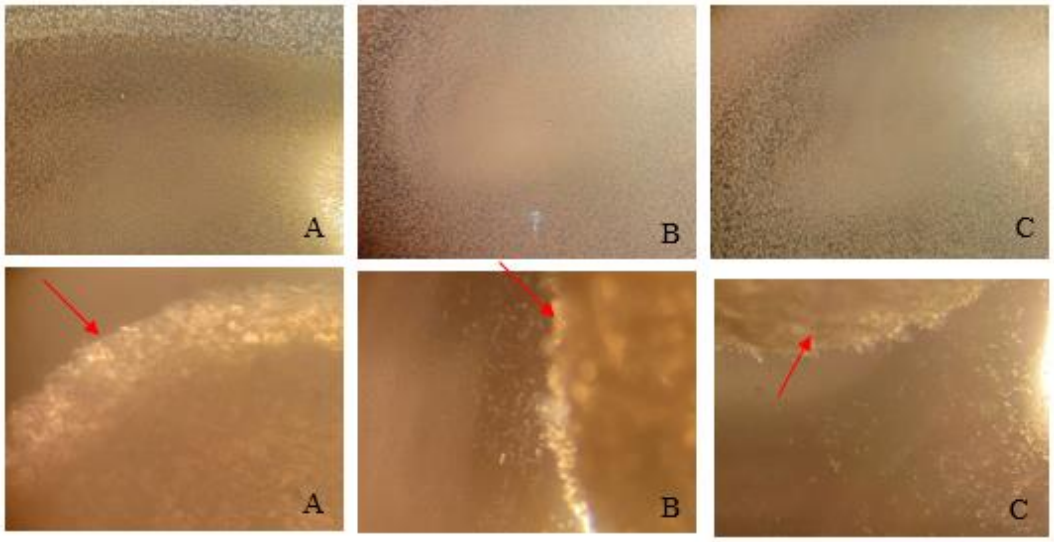

Figure 20 – Stereo microscope image of NIH3T3 cells cultured with the scaffold samples (red arrows), (a) 69:30:1, (b) 70:30:0, and (c) 70:25:5.

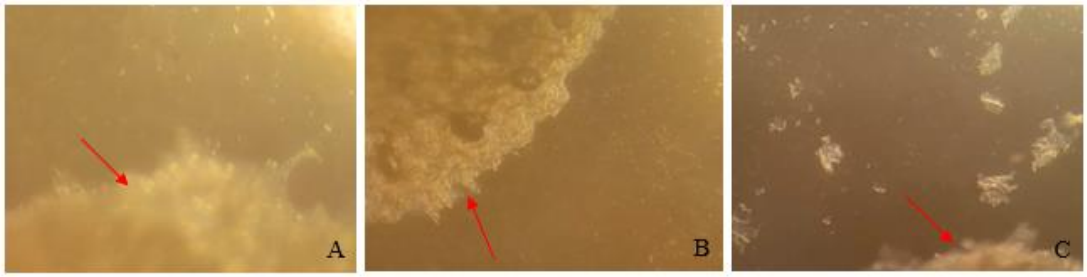

Figure 21 – Stereo microscope image of MG63 cells cultured with the scaffold samples (red arrows), (a) 69:30:1, (b) 70:30:0, and (c) 70:25:5.

The results obtained after 24 hours for NIH3T3 cells fibroblasts were 136.51% and 132.28% in samples 70:30:0 and 70:25:5, respectively, exceeding the values observed with the MG63 cells of bone origin. This difference can be explained by the higher

metabolic activity of bone cells (Vieira, 1999), which makes them more susceptible to toxins, especially in environments where intensive processes such as mineralisation and bone regeneration occur.

The results obtained for NIH3T3 and MG63 cells after 24 hours do not differ significantly from those found in the literature. In the study by Arab *et al*. (2024), a CV of 140.78 ± 11.8% was observed at 24 hours for the developed scaffolds based on Magnesium/Titanium/HAp. Furthermore, the CV of the scaffolds tested in this study was higher at 24 hours than that reported by Ghahremanzadeh *et al*. (2021), based on Polycaprolactone (PCL)/CH, which was 107.73% after 5 days. Although there has been a reduction in CV over time, the samples are still considered non-toxic, as the cell viability values remain above 70%, as established by the ISO 10993-5:2009 standard (Jung *et al*., 2019).

5 CONCLUSION AND FUTURE WORK

5.1 Conclusion

This study aimed to develop scaffolds of HAp and CH incorporated with CS for bone regeneration applications. To this end, different approaches were used to integrate CS into the scaffolds to perceive the impact on the final materials' properties.

Based on the preliminary results, it was observed that the partial or total substitution of CH, an essential component for the structural stability of the samples, makes the scaffolds fragile and brittle, leading, in some cases, to the loss of their original disc shape. Therefore, it was only possible to produce scaffolds when CH was incorporated. The scaffolds using CH and added CS at contents ranging from 1-5% showed good structural results, including maintaining the total solids content (Case B) or not (Case A) in the final dispersion.

TG analyses showed that the purification of the scaffolds by $scCO_2$ was efficient, with extraction yields varying between 55% and 100%, depending on the sample. This means the freeze-drying process combined with $scCO_2$ treatment effectively removes acetic acid, making the sample viable for biological applications. In addition, the cytotoxicity tests showed that the samples were not toxic after 48 hours.

The density analysis showed that the addition of CS to the base formulation, as developed by Ruphuy *et al*. (2017), did not substantially change or impact the density values of the scaffolds. In the swelling analysis, it was observed that the samples reached equilibrium after 10 minutes of analysis, with an initial increase in absorption followed by stabilisation of the degree of swelling. Furthermore, the addition of CS to the samples did not significantly change the absorption capacity of the scaffolds.

Finally, the scaffolds developed in this study showed great potential for application in bone regeneration, as they show no toxicity within 48 hours and exhibit low porosity, these characteristics indicate that they are suitable for applications in bone tissue. The base formulation, which mimics the composition of bone in terms of organic and inorganic components when combined with CS at different contents, highlights and emphasises the effectiveness of the produced scaffolds. Therefore, HAp/CH/CS scaffolds are promising for bone regeneration applications.

5.2 Future work

To advance research on the developed work, where HAp:CH scaffolds incorporated with CS are proposed for bone regeneration, the following activities are recommended. The first 3 are short-term objectives, and the last 3 can be seen as more long-term objectives, which will depend on the previous stages' results.

- Evaluate the controlled release profile of CS over time;
- Proceed with the mechanical analysis (DMA) of the scaffolds;
- Study of cell adhesion and proliferation for the samples of case A and case B;
- Perform the DAPI (4′,6-diamidino-2-phenylindol) test to mark and visualise DNA;
- Analysing the degradation rate of the scaffolds in vitro and in vivo;
- Test the scaffolds in animal models to assess biocompatibility, biodegradation and osteoinduction in a natural biological environment.

REFERENCES

Alcântara, S. R. C. (2011). Utilização de quitosana como biocida na agricultura em substituição aos agrotóxicos. [Dissertação de Mestrado]. Universidade Federal da Paraíba, Programa Regional de Pós-Graduação em Desenvolvimento e Meio Ambiente.

Alinejad, Y., Adoungotchodo, A., Hui, E., Zehtabi, F., & Lerouge, S. (2018). An injectable chitosan/chondroitin sulfate hydrogel with tunable mechanical properties for cell therapy/tissue engineering. *International journal of biological macromolecules*, 113, 132-141. https://doi.org/10.1016/j.ijbiomac.2018.02.069.

Amiryaghoubi, N., Fathi, M., Barar, J., & Omidi, Y. (2022). Hydrogel-based scaffolds for bone and cartilage tissue engineering and regeneration, *Reactive and Functional Polymers*. 177, 105313. https://doi.org/10.1016/j.reactfunctpolym.2022.105313.

Arab, M., Behboodi, P., Khachatourian, A. M., & Nemati, A. (2024). Enhanced mechanical properties and biocompatibility of hydroxyapatite scaffolds by magnesium and titanium oxides for bone tissue applications. *Heliyon, 10*(13). https://doi.org/10.1016/j.heliyon.2024.e33847.

Backes, E. H. (2020). Desenvolvimento de biocompósitos de poli (ácido láctico)/biocargas para impressão 3D de *scaffolds* para engenharia de tecidos ósseos. [Dissertação de Doutorado]. Universidade Federal de São Carlos, Centro de Ciências Exatas e de Tecnologia, Programa de Pós-Graduação em Ciência e Engenharia de Materiais.

Bahraminasab, M., Janmohammadi, M., Arab, S., Talebi, A., Nooshabadi, V. T., Koohsarian, P., & Nourbakhsh, M. S. (2021). Bone scaffolds: an incorporation of biomaterials, cells, and biofactors. *ACS Biomaterials Science & Engineering*, *7*(12), 5397-5431. https://doi.org/10.1021/acsbiomaterials.1c00920.

Basik, M., & Mobin, M. (2020). Chondroitin sulfate as potent green corrosion inhibitor for mild steel in 1M HCl, *Journal of Molecular Structure*. 1214, 128231. https://doi.org/10.1016/j.molstruc.2020.128231.

Beu, C. C. L., Guedes, N. L. K. O., & Quadros, Â. A. G. de. (2017). Tecido conjuntivo. Disponível em: https://www.unioeste.br/portal/microscopio-virtual/tecido-conjuntivo/especializado/osseo/celulas-e-matriz-ossea-osso-descalcificado#:~:text=A%20matriz%20%C3%B3ssea%20%C3%A9%20formada,%2C%20pot%C3%A1ssio%2C%20s%C3%B3dio%20e%20citrato. Access at: 05 dez. 2023.

Brougham, C. M., Levingstone, T. J., Shen, N., Cooney, G. M., Jockenhoevel, S., Flanagan, T. C., & O'Brien, F. J. (2017). Freeze-Drying as a Novel Biofabrication Method for Achieving a Controlled Microarchitecture within Large, Complex Natural Biomaterial Scaffolds, *Adv. Healthcare Mater*. 1700598. https://doi.org/10.1002/adhm.201700598.

Bunhack, E. J., Mendes, E. S., Pereira, N. C., & Cavalcanti, O. A. (2007). Influência do sulfato de condroitina na formação de filmes isolados de polimetacrilato: avaliação

do índice de intumescimento e permeabilidade ao vapor d'água, *Química Nova*. 30, 2, 312-317. https://doi.org/10.1590/S0100-40422007000200014.

Chan, G. R. (2016). Development of Hydroxyapatite-Based Hybrid Materials for Biomedical Applications. [Dissertação de Doutorado]. Faculdade de Engenharia, Universidade do Porto, Departamento de Engenharia Química.

Cordeiro, R. S. (2019). Biopolímeros para otimização de *scaffolds* em aplicações biomédicas: extração e caracterização. [Tese de Mestrado]. Departamento de Química, Faculdade de Ciências e Tecnologia da Universidade de Coimbra, Coimbra.

Crugeira, P. J. L., Almeida, H. H., Marcet, I., Rendueles, M., Pires, M. G., Rafael, H. M., Rodrigues, A. I. G, Santamaria-Echart, A., & Barreiro, M. F. (2023). Biosynthesis of antioxidant xanthan gum by Xanthomonas campestris using substrates added with moist olive pomace, *Food and Bioproducts Processing*. 141, 210-218. https://doi.org/10.1016/j.fbp.2023.08.008.

Cruz, D. S. da. (2021). Uso de colágeno no tratamento de doenças osteoarticulares: uma revisão integrativa. [Trabalho de Conclusão de Curso]. Centro Universitário AGES.

Cunha, M. A. da. (2010). Síntese e caracterização de hidroxiapatita nanoestruturada obtidos por aspersão de solução em chama. [Trabalho de Diplomação]. Universidade Federal do Rio Grande do Sul, Escola de Engenharias, Engenharia de Materiais.

Ewing, A. V., & Kazarian, S. G. (2018). Current trends and opportunities for the applications of in situ vibrational spectroscopy to investigate the supercritical fluid processing of polymers. The Journal of Supercritical Fluids, 134, 88-95. https://doi.org/10.1016/j.supflu.2017.12.011.

Fadeeva, I. V., Barinov, S. M., Fedotov, A. Y., & Komlev, V. S. (2012). Interactions of calcium phosphates with chitosan. In Doklady Chemistry (Vol. 441, No. 2, p. 387). 10.1134/S0012500811120044.

Farazin, A., & Ghasemi, A. H. (2022). Design, synthesis, and fabrication of chitosan/hydroxyapatite composite scaffold for use as bone replacement tissue by sol–gel method. Journal of Inorganic and Organometallic Polymers and Materials, 32(8), 3067-3082. https://doi.org/10.1007/s10904-022-02343-8.

Felipe, L. O., Rabello, L. A., Júnior, Ê. N. O., & Santos, I. J. B. (2017). Quitosana: da Química Básica à Bioengenharia, *Química e Sociedade*. 39, 4, 312-320. http://dx.doi.org/10.21577/0104-8899.20160089.

Fereshteh, Z. (2018). Freeze-drying technologies for 3D scaffold engineering, *Materials, Technologies and Applications*. Pages 151-174. https://doi.org/10.1016/B978-0-08-100979-6.00007-0.

Fernandes, L. L. (2009). Produção e caracterização de membranas de quitosana e quitosana com sulfato de condroitina para aplicações biomédicas. [Trabalho de Conclusão de Curso]. Universidade Federal do Rio de Janeiro, Departamento de Engenharia Metalúrgica e de Materiais.

Ferrari, A. J. L. (2016). O uso de condroitina e glucosamina no tratamento da osteoartrite. *Rev Paul Reumatol*. 15, 16-20. https://doi.org/10.46833/reumatologiasp.2016.15.1.16-20.

Flores, M. A. R., Barbosa, W. T., Gonçalves, A. P. B., Vieira, J. L., Soares, M. B. P., & Barbosa, J. D. V. (2023). Desenvolvimento de *scaffolds* combinando a técnica de bioimpressão 3D e eletrofiação para uso na engenharia de tecidos: uma revisão bibliográfica. Anuário de resumos expandidos apresentados no VIII SAPCT - SENAI CIMATEC. ISSN 0805-2010.

Fourie, J., Taute, F., du Preez, L., & De Beer, D. (2022). Chitosan composite biomaterials for bone tissue engineering—a review. *Regenerative Engineering and Translational Medicine*, 1-21. https://doi.org/10.1007/s40883-020-00187-7.

Georgieva, V., Zvezdova, D., & Vlaev, L. (2012). Non-isothermal kinetics of thermal degradation of chitosan. Chemistry Central Journal, 6, 1-10. https://doi.org/10.1186/1752-153X-6-81.

Ghahremanzadeh, F., Alihosseini, F., & Semnani, D. (2021). Investigation and comparison of new galactosylation methods on PCL/chitosan scaffolds for enhanced liver tissue engineering. *International Journal of Biological Macromolecules*, *174*, 278-288. https://doi.org/10.1016/j.ijbiomac.2021.01.158.

Gritsch, L., Maqbool, M., Mouriño, V., Ciraldo, F. E., Cresswell, M., Jackson, P. R., Lovell, C. & Boccaccini, A. R. (2019). Chitosan/hydroxyapatite composite bone tissue engineering scaffolds with dual and decoupled therapeutic ion delivery: Copper and strontium. Journal of Materials Chemistry B, 7(40), 6109-6124. https://doi.org/10.1039/C9TB00897G.

Guo, L., Chen, H., Li, Y., Zhou, J., & Chen, J. (2023). Biocompatible scaffolds constructed by chondroitin sulfate microspheres conjugated 3D-printed frameworks for bone repair, *Carbohydrate Polymers*. 299, 120188. https://doi.org/10.1016/j.carbpol.2022.120188.

Hu, Y., Chen, J., Fana, T., Zhanga, Y., Zhaoa, Y., Shib, X., & Zhang, Q. (2017). Biomimetic mineralized hierarchical hybrid scaffolds based on in situ synthesis of nano-hydroxyapatite/chitosan/chondroitin sulfate/hyaluronic acid for bone tissue engineering, *Colloids and Surfaces B: Biointerfaces*. 157, 93–100. http://dx.doi.org/10.1016/j.colsurfb.2017.05.059.

Huang, L., Sui, W., Wang, Y., & Jiao, Q. (2010). Preparation of chitosan/chondroitin sulfate complex microcapsules and application in controlled release of 5-fluorouracil, *Carbohydrate Polymers*. 80, 168–173. doi:10.1016/j.carbpol.2009.11.007.

Janek, M., Vašková, I., Pischová, M., Fialka R., Hajdúchová, Z., Veteška, P., Feranc, J., Orlovská, M. H., Peciar, P., Rakovský, E., & Bača, Ľ. (2024). Characteristics of sintered calcium deficient hydroxyapatite scaffolds produced by 3D printing, *Journal of the European Ceramic Society*. 44, 9, 5284-5297. https://doi.org/10.1016/j.jeurceramsoc.2024.01.047.

Jardim, K. V., Lima, L. A., Parize, A. L., Sousa, M. H., & Chaker, J. A. (2012). Caracterização dos parâmetros de obtenção de nanopartículas de quitosana/sulfato de

condroítina usadas na encapsulação da curcumina. 52° Congresso Brasileiro de Química. https://www.abq.org.br/cbq/2012/trabalhos/8/681-14451.html.

Jung, O., Smeets, R., Hartjen, P., Schnettler, R., Feyerabend, F., Klein, M., ... & Kopp, A. (2019). Improved in vitro test procedure for full assessment of the cytocompatibility of degradable magnesium based on ISO 10993-5/-12. *International Journal of Molecular Sciences*, *20*(2), 255. http://dx.doi.org/10.3390/ijms20020255.

Kakazu, D. A., & Malmonge, S. M. (2014). Scaffolds de quitosana para engenharia tecidual neural. XXIV Congresso Brasileiro de Engenharia Biomédica – CBEB 2014. http://dx.doi.org/10.13140/RG.2.1.1706.0003.

Laranjeira, M. C. M., & Fávere, V. T. de. (2009). Quitosana: biopolímero funcional com potencial industrial biomédico, *Química Nova*. 32, 3, 672-678. https://doi.org/10.1590/S0100-40422009000300011.

Ma, P., Wu, W., Wei, Y., Ren, L., Lin, S., & Wu, J. (2021). Biomimetic gelatin/chitosan/polyvinyl alcohol/nano-hydroxyapatite scaffolds for bone tissue engineering, *Materials & Design*. 207, 109865. https://doi.org/10.1016/j.matdes.2021.109865.

Manjare, S. D., & Dhingra, K. (2019). Supercritical fluids in separation and purification: A review. *Materials Science for Energy Technologies*, *2*(3), 463-484. https://doi.org/10.1016/j.mset.2019.04.005.

Miri, Z., Haugen, H. J., Loca, D., Rossi, F., Perale, G., Moghanian, A., & Ma, Q. (2024). Review on the strategies to improve the mechanical strength of highly porous bone bioceramic *scaffolds*, *Journal of the European Ceramic Society*. 44, 23–42. https://doi.org/10.1016/j.jeurceramsoc.2023.09.003.

Mohammadi, N., Amnieh, Y. A., Ghasemi, S., Karbasi, S., & Vaezifar, S. (2024). Evaluation of the effects of decellularized extracellular matrix nanoparticles incorporation on the polyhydroxybutyrate/nano chitosan electrospun scaffold for cartilage tissue engineering. *International Journal of Biological Macromolecules*, 133217. https://doi.org/10.1016/j.ijbiomac.2024.133217.

Moniz, K. A. D. (2015). Efeitos da glucosamina e sulfato de condroitina na osteoclastogénese humana. [Dissertação de Mestrado]. Universidade do Porto, Faculdade de Farmácia.

Mosmann, T. (1983). Rapid colorimetric assay for cellular growth and survival: application to proliferation and cytotoxicity assays. *Journal of immunological methods*, *65*(1-2), 55-63. https://doi.org/10.1016/0022-1759(83)90303-4.

Nakano, F. P. (2016). Obtenção de microesferas quitosana/taninos extraídos da casca de Eucalyptus urograndis para utilização piloto na tratabilidade físico-química de água bruta com turbidez entre 100-110 NTU. [Dissertação de Mestrado]. Universidade de São Paulo, Escola de Engenharia de Lorena.

Nakano, T., Betti, M., & Pietrasik, Z. (2010). Extraction, isolation and analysis of chondroitin sulfate glycosaminoglycans, *Recent Patents on Food, Nutrition & Agriculture*. 2, 61-74. DOI: 10.2174/2212798411002010061

O'brien, F. J. (2011). Biomaterials & scaffolds for tissue engineering. *Materials today*, 14(3), 88-95. https://doi.org/10.1016/S1369-7021(11)70058-X.

Oliveira, A. P. V., de Abreu Feitosa, V., de Oliveira, J. M., Coelho, A. L., Lídia de Araújo, P. V., da Silva, F. D. A. R., ... & de Souza, B. W. (2017). Characteristics of chondroitin sulfate extracted of tilapia (Oreochromis niloticus) processing. Procedia engineering, 200, 193-199. https://doi.org/10.1016/j.proeng.2017.07.028.

Pavão, M. S. G., Vilela-Silva, A. C., & Mourão, P. A. S. (2006). Biosynthesis of Chondroitin Sulfate: From the Early, Precursor Discoveries to Nowadays, Genetics Approaches, *Advances in Pharmacology*. 53, 117-140. DOI: 10.1016/S1054-3589(05)53006-0.

Plikus, M. V., Wang, X., Sinha, S., Forte, E., Thompson, S. M., Herzog, E. L., ... & Horsley, V. (2021). Fibroblasts: Origins, definitions, and functions in health and disease. *Cell*, *184*(15), 3852-3872. https://doi.org/10.1016/j.cell.2021.06.024.

Pomin, V. (2013). Condroitim sulfato: estrutura, uso e implicações na saúde. Disponível em: Condroitim sulfato: estrutura, uso e implicações na saúde - IBqM (ufrj.br). Acesso em: 26 jan. 2024.

Rezende, M. U., Campos, G. C., & Pailo, A. F. (2013). Conceitos atuais em osteoartrite. *Acta Ortop Bras*. 21, 120-122. http://www.scielo.br/aob.

Rstakyan, V., Mkhitaryan, L., Baghdasaryan, L., Ghaltaghchyan, T., Karabekian, Z., Sevoyan, G., Aghayan, M., & Rodríguez, M. A. (2024). Stereolithography of ceramic scaffolds for bone tissue regeneration: Influence of hydroxyapatite/silica ratio on mechanical properties, *Journal of the Mechanical Behavior of Biomedical Materials*. 152, 106421. https://doi.org/10.1016/j.jmbbm.2024.106421.

Ruphuy, G., Lopes, J. C., Dias, M. M., & Barreiro, M. F. (2019). New insights into nanohydroxyapatite/chitosan nanocomposites for bone tissue regeneration, *Materials for Biomedical Engineering: Nanobiomaterials in Tissue Engineering*. pp. 331-371. https://doi.org/10.1016/B978-0-12-816909-4.00011-7.

Ruphuy, G., Saralegi, A., Lopes, J. C., Dias, M. M., & Barreiro, M. F. (2016). Spray drying as a viable process to produce nano-hydroxyapatite/chitosan (n-HAp/CS) hybrid microparticles mimicking bone composition, *Advanced Powder Technology*. 27, 575–583. http://dx.doi.org/10.1016/j.apt.2016.02.010.

Ruphuy, G., Souto-Lopes, M., Paiva, D., Costa, P., Rodrigues, A. E., Monteiro, F. J., Salgado, C. L., Fernandes, M. H., Lopes, J. C., Dias, M. M., Barreiro, M. F. (2018). Supercritical CO_2 assisted process for the production of high-purity and sterile nano-hydroxyapatite/chitosan hybrid scaffolds. *Journal of Biomedical Materials Research Part B: Applied Biomaterials*, *106*(3), 965-975. https://doi.org/10.1002/jbm.b.33903.

Sanches, S. C. C. (2013). Caracterização físico-química e avaliação toxicológica preliminar do copolímero sulfato de condroitina-co-n-isopropilacrilamida para uso farmacêutico. [Dissertação de Mestrado]. Universidade Federal do Pará, Instituto de Ciências da Saúde.

Santos, C. V. dos. (2009). Sulfato de condroitina: da matéria-prima a terapêutica. [Trabalho de Conclusão de Curso]. Universidade Federal do Rio Grande do Sul, Faculdade de Veterinária.

Schreiner, T. B., Colucci, G., Santamaria-Echart, A., Fernandes, I. P., Dias, M. M., Pinho, S. P., & Barreiro, M. F. (2021). Evaluation of saponin-rich extracts as natural alternative emulsifiers: A comparative study with pure Quillaja Bark saponin, *Colloids and Surfaces A: Physicochemical and Engineering Aspects*. 623, 126748. https://doi.org/10.1016/j.colsurfa.2021.126748.

Szustakiewicz, K., Włodarczyk, M., Gazińska, M., Rudnicka, K., Płociński, P., Szymczyk-Ziółkowska, P., ... & Trochimczuk, A. W. (2021). The effect of pore size distribution and l-lysine modified apatite whiskers (Hap) on osteoblasts response in plla/hap foam scaffolds obtained in the thermally induced phase separation process. International journal of molecular sciences, 22(7), 3607. https://doi.org/10.3390/ijms22073607.

Teixeira, B. I. B. (2016). Preparação e caraterização de scaffolds de colagénio-nanohidroxiapatite modificados com *O-phospho-L-serine* para a regeneração tecidular óssea. [Tese de Mestrado]. Universidade Católica Portuguesa, Portugal.

UNIRIO. (2020). *Doenças crônicas não transmissíveis: doenças ósseas*. Setor de Alimentação e Nutrição, Pró-Reitoria de Assuntos Estudantis. Boletim nº 15.

Valentim, R. M. B., Andrade, S. M. C., Santos, M. E. M. dos., Santos, A. C., Pereira, V. S., Santos, I. P. dos., Dias, C. G. B. T., & Reis. M. A. L. dos. (2018). Composite based on biphasic calcium phosphate (HA/β-TCP) and nanocellulose from the açaí tegument, *Materials*. 11, 2213. doi:10.3390/ma11112213.

Venkatesan, J., Pallela, R., Bhatnagara, I., & Kim, S. K. (2012). Chitosan-amylopectin/hydroxyapatite and chitosan-chondroitin sulphate/hydroxyapatite composite scaffolds for bone tissue engineering, *International Journal of Biological Macromolecules*. 51, 1033-1042. http://dx.doi.org/10.1016/j.ijbiomac.2012.08.020.

Vieira, J. G. H. (1999). Considerações sobre os marcadores bioquímicos do metabolismo ósseo e sua utilidade prática. *Arquivos Brasileiros de Endocrinologia & Metabologia*, *43*, 415-422. https://doi.org/10.1590/S0004-27301999000600005.

Wang, C., Wang, H., Chen, Q., Gang, H., Zhou, Y., Gu, S., Liu, X., Xu, W., Zhang B., & Yang, H. (2022). Polylactic acid scaffold with directional porous structure for large-segment bone repair, *International Journal of Biological Macromolecules*. 216, 810–819. https://doi.org/10.1016/j.ijbiomac.2022.07.207.

Wang, J., Duan, X., Zhong, D., Zhang, M., Li, J., Hu, Z., & Han, F. (2024). Pharmaceutical applications of chitosan in skin regeneration: A review, *International Journal of Biological Macromolecules*. 261, 129064. https://doi.org/10.1016/j.ijbiomac.2023.129064.

Wang, X., Wang, B., Liu, W., Yu, D., Song, Z., Li, G., Liu, X., Wang, H., & Ge, S. (2024). Using chitosan nanofibers to simultaneously improve the toughness and sensing performance of chitosan-based ionic conductive hydrogels, *International Journal of Biological Macromolecules*. 260, 129272. https://doi.org/10.1016/j.ijbiomac.2024.129272.

Wang, Y., Zhang, Y., Liu, X., Sun, S., & Chen, B. (2024). Design of amidoximized hydroxyapatite for extracting uranium from seawater. Radiation Physics and Chemistry, *Radiation Physics and Chemistry*. 217, 111512. https://doi.org/10.1016/j.radphyschem.2024.111512.

White, M. T., Bianchi, G., Chai, L., Tassou, S. A., & Sayma, A. I. (2021). Review of supercritical CO2 technologies and systems for power generation. *Applied Thermal Engineering*, *185*, 116447. https://doi.org/10.1016/j.applthermaleng.2020.116447.

Xu, C., Liu, Z., Chen, X., Gao, Y., Wang, W., Zhuang, X., Zhang, H., & Dong, X. (2024). Bone tissue engineering scaffold materials: Fundamentals, advances, and challenges, *Chinese Chemical Letters*. 35, 109197. https://doi.org/10.1016/j.cclet.2023.109197.

Xu, D., Xu, Z., Cheng, L., Gao, X., Sun, J., & Chen, L. (2022). Improvement of the mechanical properties and osteogenic activity of 3D-printed polylactic acid porous scaffolds by nano-hydroxyapatite and nano-magnesium oxide, *Heliyon*. 8, e09748. https://doi.org/10.1016/j.heliyon.2022.e09748.

Xu, K., Wang, Z., Copland, J. A., Chakrabarti, R., & Florczyk, S. J. (2020). 3D porous chitosan-chondroitin sulfate *scaffolds* promote epithelial to mesenchymal transition in prostate cancer cells, *Biomaterials*. 254, 120126. https://doi.org/10.1016/j.biomaterials.2020.120126.

Xu, L., Ma, F., Leung, F. K. L., Qin, C., Lu, W. W., & Tang, B. (2021). Chitosan-strontium chondroitin sulfate *scaffolds* for reconstruction of bone defects in aged rats, *Carbohydrate Polymers*. 273, 118532. https://doi.org/10.1016/j.carbpol.2021.118532.

Yan, S., Zhang, Q., Wang, J., Liu, Y., Lu, S., Li, M., & Kaplan, D. L. (2013). Silk fibroin/chondroitin sulfate/hyaluronic acid ternary *scaffolds* for dermal tissue reconstruction, *Acta Biomaterialia*. 9, 6771–6782. http://dx.doi.org/10.1016/j.actbio.2013.02.016.

Yang, K. C., Yang, Y. T., Wu, C. C., Hsiao, J. K., Huang, C. Y., Chen, I. H., & Wang, C. C. (2023). Bioinspired collagen-gelatin-hyaluronic acid-chondroitin sulfate tetra-copolymer scaffold biomimicking native cartilage extracellular matrix facilitates chondrogenesis of human synovium-derived stem cells, *International Journal of Biological Macromolecules*. 240, 124400. https://doi.org/10.1016/j.ijbiomac.2023.124400.

Yu, Z., Yu, D., Dong, J., & Xia, W. (2022). Ultrasound-reinforced encapsulation of proanthocyanidin by chitosan-chondroitin sulfate nanosystem, *Food Hydrocolloids*. 132, 107872. https://doi.org/10.1016/j.foodhyd.2022.107872.

Zhou, L., Fanc, L., Zhanga, F. M., Jiangd, Y., Caie, M., Daia, C., Luoa, Y. A., Tua, L. J., Zhoua, Z. N., Lia, X. J., Ning, C. Y., Zheng, K., Boccaccini, A. R., & Tan, G. X.

(2021). Hybrid gelatin/oxidized chondroitin sulfate hydrogels incorporating bioactive glass nanoparticles with enhanced mechanical properties, mineralization, and osteogenic differentiation, *Bioactive Materials*. 6, 890–904. https://doi.org/10.1016/j.bioactmat.2020.09.012.

APPENDIX A

A.1 Preparation of the dispersions (Case A and Case B)

The masses used to prepare the samples for Cases A and B are shown in Table A.1.

Table A.1 – Masses used to prepare the samples for Cases A and B.

CASE A				
Sample	**HAp paste (g)**	**CH solution (g)**	**Buffer (g)**	**CS (g)**
A.1%	13.47	28.86	57.67	0.0291
A.2.5%	13.47	28.86	57.67	0.0740
A.5%	13.47	28.86	57.67	0.1519
CASE B				
Sample	**HAp paste (g)**	**CH solution (g)**	**Buffer (g)**	**CS (g)**
B.1%	13.33	28.57	58.10	0.0289
B.2.5%	13.13	28.14	58.73	0.0721
B.5%	12.79	27.41	59.79	0.1443

A.2 Complete degradation stages and corresponding mass loss for Preliminary Tests and Case A

The complete degradation stages and corresponding mass loss for Preliminary Tests and Case A are presented in Table A.2.

Table A.2 – Complete degradation stages and corresponding mass loss for Preliminary Tests and Case A.

Sample	Degradation Temperature (°C)	Weigh Loss (%)	Residue (%)
70.30.0_SC	63 - 251.8	13.37 - 24.13	62.29
70.30.0	52.7 138.6 246.9	6.75 2.27 16.42	73.88
70.25.5_SC	61.7 186.4 249	7.22 2.11 16.92	72.71
70.25.5	56.1 140.2 260.1	8.29 5.14 16.22	72.43
69.30.1_SC	54.2 - 248.4	6.43 - 20.86	68.11
69.30.1	61.7 134.7 248.9	7.79 4.03 19.18	68.74
A.1%	60.4 127.4 246.9 411.4	13.75 4.12 16.01 5.83	68.39%
A.1% - SC	68.9 - 245.6 444.4	18.47 - 18.38 8.52	56.95%
A.2.5%	65.1 135.9 255.2 405.5	10.08 6.64 16.78 6.78	62.58%
A.2.5% - SC	69.1 164.5 257.3 431.6	10.3 1.84 14.93 6.4	69.82%
A.5%	69.1 154.9 261.4 395.4	13.59 6.09 16.17 6.32	64.49%
A.5% - SC	68.4 186.9 257.4 433.9	10.25 2.71 15.12 6.14	69.82%

APPENDIX B

Participation in Congress

This work has been accepted as a poster for the International Meeting of XXVIII Encontro Galego-Portugués de Química.

Development of Chondroitin Sulfate-loaded Chitosan/Hydroxyapatite Scaffolds Targeting Bone Regeneration

Júlia Pissaia[1,4], Tatiana B. Schreiner[1], Yaidelin Manrique[2,3], Elisângela Düsman[4], Maria Filomena Barreiro[1], Arantzazu Santamaria-Echart[1,*]
[1]CIMO, LA SusTEC, Instituto Politécnico de Bragança, Campus de Santa Apolónia, 5300-253 Bragança, Portugal
[2]LSRE-LCM - Laboratory of Separation and Reaction Engineering–Laboratory of Catalysis and Materials, Faculdade de Engenharia, Universidade do Porto, Rua Dr. Roberto Frias, Porto, 4200-465, Portugal
[3]ALiCE - Associate Laboratory in Chemical Engineering, Faculty of Engineering, University of Porto, Rua Dr. Roberto Frias, 4200-465 Porto, Portugal
[4]Department of Chemistry and Biology, Universidade Tecnológica Federal do Paraná (UTFPR), Campus Francisco Beltrão, Francisco Beltrão, Paraná, Brazil
asantamaria@ipb.pt, http://cimo.ipb.pt

Bone tissue has a high capacity for healing, but large-size defects require intervention [1]. Chondroitin sulphate (CS) can create a favourable environment for growth factors, which can help tissue repair. This makes CS an attractive option to combine with artificial scaffolds, like chitosan/hydroxyapatite (CH/HAp) scaffolds. These scaffolds mimic bone composition and are gradually resorbed by the body, facilitating natural regeneration without requiring surgical removal [2].

In this study, scaffolds were prepared using 30% of CH (organic component) and 70% of HAp (inorganic component), mimicking the typical bone organic:inorganic ratio (30:70) [3]. Different concentrations of CS were tested, maintaining the HAp concentration fixed. The prepared samples are shown in Fig. 1. Supercritical CO_2 ($scCO_2$) was used to remove the acetic acid introduced for CH solubilisation. The samples were characterised by thermal analysis (TG), density, and swelling to assess scaffold structure and composition, targeting future cell adhesion and biocompatibility tests. TG results confirmed that scCO2 effectively removed the acid, ensuring the biological viability of the scaffolds. The density values (~0.05 g/cm³) and swelling capacities (2.79–3.24 g/g) were consistent with literature data. Overall, the CS-incorporated scaffolds are promising materials for bone regeneration.

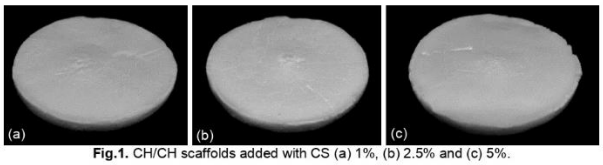

Fig.1. CH/CH scaffolds added with CS (a) 1%, (b) 2.5% and (c) 5%.

Acknowledgements
FCT for financial support through national funds FCT/MCTES (PIDDAC) to CIMO UIDB/00690/2020 (DOI:10.54499/UIDB/00690/2020) and UIDP/00690/2020 (DOI:10.54499/UIDP/00690/2020); SusTEC LA/P/0007/2020 (DOI:10.54499/LA/P/0007/2020); LSRE-LCM UIDB/50020/2020 (DOI:10.54499/UIDB/50020/2020) and UIDP/50020/2020 DOI:10.54499/UIDP/50020/2020); and ALiCE LA/P/0045/2020 (DOI:10.54499/LA/P/0045/2020). The UTFPR and the Araucária Foundation for PD&I Agreement nº. 429/2022 and to the National Council for Scientific and Technological Development (CNPq#305029/2022-3).

References
[1] N. Amiryaghoubi, M. Fathi, J. Barar, Y. Omidi, Reactive and Functional Polymers 177 (2012) 105313.
[2] L. Guo, H. Chen, Y. Li, J. Zhou, J. Chen, Carbohydrate Polymers, 299 (2023) 120188.
[3] G. Ruphuy, M. Souto-Lopes, D. Paiva, P. Costa, A. E. Rodrigues, F. J. Monteiro, C. L. Salgado, M. H. Fernandes, J. C. Lopes, M. M. Dias, M. F. Barreiro, Journal of Biomedical Materials Research Part B: Applied Biomaterials 106 (2018) 965-975.

COMUNICACIÓN ACEPTADA

De Secretaria Colegio de Químicos
Para tatianas@ipb.pt
Data Hoje 07:46
Resumo Cabeçalhos Texto simples

Buenos días,

Le informamos que su comunicación titulada ***"Development of Chondroitin Sulfate-loaded Chitosan/Hydroxyapatite Scaffolds Targeting Bone Regeneration"*** ha sido admitida para su presentación en el XXVIII Encontro Galego Portugués de Química en formato ***"Poster"***

En caso de haber solicitado la factura con reducción **y aún no haber enviado los justificantes** de socios SPQ, Estudiante de grado, máster, doctorado o postdoctorado, debes enviarlos cuanto antes para la emisión de la factura. En caso de no recibirlos, la factura será por 260 €.

Saludos
Comisión de organización